International Journal of Heat and Mass Transfer 58 (2013) 718–734

Contents lists available at SciVerse ScienceDirect

International Journal of Heat and Mass Transfer

journal homepage: www.elsevier.com/locate/ijhmt

Universal approach to predicting two-phase frictional pressure drop for mini/micro-channel saturated flow boiling

Sung-Min Kim, Issam Mudawar *

Boiling and Two-Phase Flow Laboratory (BTPFL), Purdue University International Electronic Cooling Alliance (PUIECA), Mechanical Engineering Building, 585 Purdue Mall, West Lafayette, IN 47907-2088, USA

ARTICLE INFO

Article history:
Received 22 April 2012
Received in revised form 6 November 2012
Accepted 14 November 2012
Available online 23 December 2012

Keywords:
Pressure drop
Flow boiling
Evaporation
Mini-channel
Micro-channel

ABSTRACT

This paper is a part of a recent series of studies by the authors to develop universal predictive tools for pressure drop and heat transfer coefficient for mini/micro-channel flows that are capable of tackling fluids with drastically different thermophysical properties and very broad ranges of all geometrical and flow parameters of practical interest. In this study, a new technique is proposed to predict the frictional pressure gradient for saturated flow boiling. To both develop and validate the new technique, a consolidated database consisting of 2378 data points is amassed from 16 sources. The database consists of 9 working fluids, hydraulic diameters from 0.349 to 5.35 mm, mass velocities from 33 to 2738 kg/m^{2}s, liquid-only Reynolds numbers from 156 to 28,010, qualities from 0 to 1, reduced pressures from 0.005 to 0.78, and both single-channel and multi-channel data. Careful examination of many prior models and correlations shows clear differences in frictional pressure gradient predictions between non-boiling (adiabatic and condensing) versus boiling mini/micro-channel flows that are caused by differences in flow structure, especially droplet entrainment effects. A separated flow technique previously developed by the authors for non-boiling mini/micro-channel flows is modified to account for these differences. The new technique shows very good predictions of the entire consolidated database, evidenced by an overall MAE of 17.2% and even predictive accuracy for different working fluids, and over broad ranges of hydraulic diameter, mass velocity, quality and pressure, and for both single and multiple mini/micro-channels.

1. Introduction

In the early days of electronic device development, tackling heat removal used to be an afterthought since power densities were miniscule and the heat removal could therefore be handled by rather simple natural or forced air convection techniques. As power densities began to escalate appreciably during the 1980s, device developers were confronted with a new reality where the heat removal became an integral part of the design process. The recent developments in applications such as high performance computers, electrical vehicle power electronics, avionics, and directed energy laser and microwave weapon systems, have led to unprecedented increases in power density, rendering obsolete all air cooling and even some of the most aggressive single-phase liquid cooling schemes. These increases necessitated a transition to two-phase cooling schemes, which capitalize upon the coolant's latent heat content to achieve orders of magnitude enhancement in boiling and condensation heat transfer coefficients [1]. Two-phase cooling solutions come in a variety of configurations, including pool boiling [2], spray [3–5], jet [6–9], and mini/micro-channel [2,10–13], as well as surface enhancement techniques [14].

Of the many phase-change cooling options, two-phase mini/micro-channel heat sinks have gained the most popularity among device and system manufacturers because of a number of attributes, including simple construction, compactness, low coolant inventory, and ability to achieve very large heat transfer coefficients. The attractive thermal performance of two-phase mini/micro-channel heat sinks is largely the result of small coolant passage diameter. Unfortunately, small diameter can also be the cause for high pressure drop, which may comprise the efficiency of the entire cooling system. Therefore, the design of high performance mini/micro-channel heat sinks demands accurate predictive tools for both pressure drop and boiling heat transfer coefficient.

Recently, the authors of the present study proposed that pressure drop predictive models and correlations for mini/micro-channel flows must address fundamental differences in flow structure between flow boiling on one hand and condensing and adiabatic flows on the other [15]. As illustrated in Fig. 1(a), this difference is manifest in the existence of entrained droplets in the vapor core for boiling flows and their absence from both condensing and adiabatic flows. For flow boiling in micro-channels, bubbles coalesce very quickly in the upstream region of the channel, causing rapid

* Corresponding author. Tel.: +1 765 494 5705; fax: +1 765 494 0539.
E-mail address: mudawar@ecn.purdue.edu (I. Mudawar).
URL: https://engineering.purdue.edu/BTPFL (I. Mudawar).

0017-9310/$ - see front matter © 2012 Elsevier Ltd. All rights reserved.
http://dx.doi.org/10.1016/j.ijheatmasstransfer.2012.11.045

Nomenclature

Bd	Bond number
Bd^*	modified Bond number
Bo	Boiling number, q''_H/Gh_{fg}
C	parameter in Lockhart–Martinelli correlation
D	tube diameter
D_h	hydraulic diameter
Fr	Froude number
f	Fanning friction factor
G	mass velocity
g	gravitational acceleration
h_{fg}	latent heat of vaporization
J_f	superficial liquid velocity, $J_f = G(1-x)/\rho_f$
J_g	superficial vapor velocity, $J_g = Gx/\rho_g$
L	length
MAE	mean absolute error
N	number of data points
N_{conf}	Confinement number
P	pressure
P_{atm}	atmospheric pressure
P_{crit}	critical pressure
P_F	wetted perimeter of channel
P_H	heated perimeter of channel
P_R	reduced pressure, $P_R = P/P_{crit}$
ΔP	pressure drop
q''_H	heat flux based on heated perimeter of channel
Re	Reynolds number
Re_f	superficial liquid Reynolds number, $Re_f = G(1-x)D_h/\mu_f$
Re_{fo}	liquid-only Reynolds number, $Re_{fo} = GD_h/\mu_f$
Re_g	superficial vapor Reynolds number, $Re_g = GxD_h/\mu_g$
Re_{go}	vapor-only Reynolds number, $Re_{go} = GD_h/\mu_g$
Su	Suratman number
v	specific volume
v_{fg}	specific volume difference between saturated vapor and saturated liquid
We	Weber number
X	Lockhart–Martinelli parameter
x	thermodynamic equilibrium quality
z	stream-wise coordinate

Greek symbols

α	void fraction
β	channel aspect ratio ($\beta < 1$)
θ	percentage predicted within ±30%
λ	mean absolute error
μ	dynamic viscosity
ξ	percentage predicted within ±50%
ρ	density
$\bar{\rho}$	mixture density
σ	surface tension
ϕ	two-phase multiplier; channel inclination angle

Subscripts

A	accelerational
exp	experimental (measured)
F	frictional
f	saturated liquid
fo	liquid only
G	gravitational
g	saturated vapor
go	vapor only
k	liquid (f) or vapor (g)
$pred$	predicted
sat	saturation
tp	two-phase
tt	turbulent liquid-turbulent vapor
tv	turbulent liquid-laminar vapor
vt	laminar liquid-turbulent vapor
vv	laminar liquid-laminar vapor

transition to annular flow, and liquid shattered from upstream forms small droplets that are entrained in the vapor core [16]. This behavior is evident from video images in Fig. 1(b), which show micro-channel walls sheathed with a thin liquid film, with droplets clearly entrained in the vapor core [17]. However, recent images of annular condensing flow in micro-channels, which are also depicted in Fig. 1(b), show no evidence of droplet entrainment in the vapor core [15]. Clearly, different predictive tools must be developed for pressure drop in boiling flows compared to those for condensing and adiabatic flows.

Researchers have used different approaches with various levels of complexity to predict flow boiling pressure drop in mini/micro-channels [18–33]. These approaches can be grouped mostly into two general categories, those that are based on the homogeneous equilibrium model [34–40] and those that utilize semi-empirical correlations [41–57].

But there are also a few theoretical models for two-phase pressure drop. Being the most prevalent in mini/micro-channels, annular flow has been the target of more theoretical modeling efforts than all other flow regimes combined. These modeling efforts rely mostly on the control volume approach, where conservation relations are applied separately to the liquid and vapor phases. This approach has shown great versatility in tackling a wide variety of two-phase flow configurations, including pool boiling [58,59], vertical separated flow boiling along short walls [60,61] and long heated walls [62–65], in addition to annular condensation in mini/micro-channels [66].

Only a few prior studies have explored the development of a generalized predictive approach for flow boiling pressure drop in mini/micro-channels that is suitable for all possible flow boiling regimes [54–57]. In fact, no accurate predictive tools presently exit that can tackle a wide range of working fluids, mass velocities, pressures, and channel diameters. The development of this type of predictive tool is the primary motivation for a series of studies that have been initiated at the Purdue University Boiling and Two-Phase Flow Laboratory (PU-BTPFL), which involve systematic consolidation of world databases for condensation and flow boiling in mini/micro-channels, and development of universal predictive tools for both pressure drop and heat transfer coefficient, following very closely a methodology that was adopted earlier at PU-BTPFL to predict flow boiling critical heat flux (CHF) for water flow in tubes [67–70].

Recently, the authors of the present study used this approach to develop a universal predictive tool for pressure drop in condensing and adiabatic mini/micro-channel flows [71], which showed high accuracy in predicting data spanning very broad ranges of all key flow parameters. The present study follows the same systematic methodology to develop a universal approach to predicting pressure drop for flow boiling in mini/micro-channels. To accomplish this goal, flow boiling pressure drop databases are amassed from 16 sources into a single consolidated database. The database is compared to predictions of previous homogeneous equilibrium models and semi-empirical correlations for both macro-channels and mini/micro-channels. A new universal correlation for

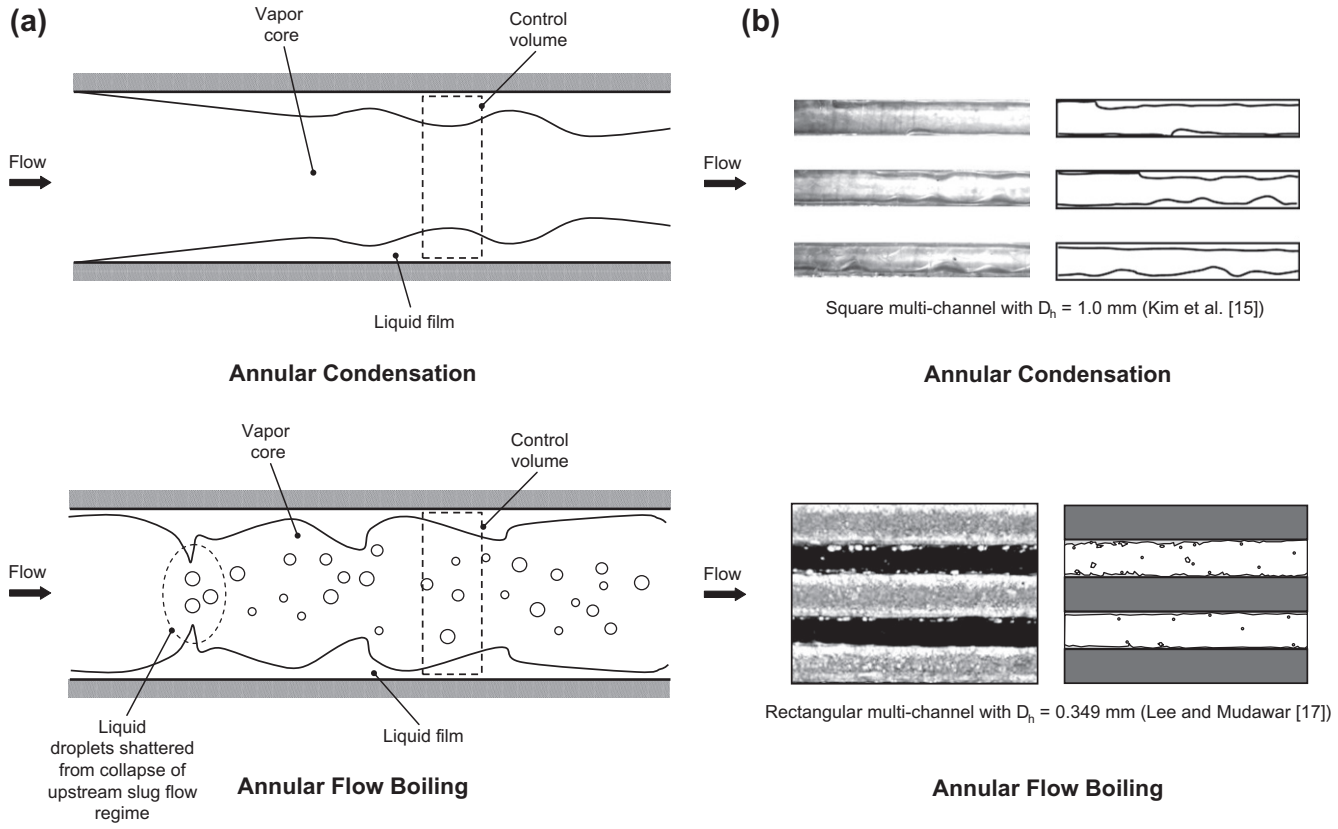

Fig. 1. (a) Fundamental differences between annular condensation (also annular adiabatic flow, on a local basis) and annular flow boiling in mini/micro-channels [15]. (b) Representative photographs (left) and schematics (right) of annular condensing [15] and annular boiling [17] flow regimes.

two-phase frictional pressure drop is derived and its accuracy validated over broad ranges of operating conditions and many working fluids.

2. Previous predictive two-phase pressure drop methods

The two-phase pressure drop can be expressed as the sum of frictional, gravitational and accelerational components,

$$\Delta P_{tp} = \Delta P_{tp,F} + \Delta P_{tp,G} + \Delta P_{tp,A}. \tag{1}$$

The accelerational pressure gradient can be expressed as

$$-\left(\frac{dP}{dz}\right)_A = G^2 \frac{d}{dz}\left[\frac{\upsilon_g x^2}{\alpha} + \frac{\upsilon_f (1-x)^2}{(1-\alpha)}\right], \tag{2}$$

where the void fraction, α, is expressed in terms of flow quality, x, using Zivi's correlation [72],

$$\alpha = \left[1 + \left(\frac{1-x}{x}\right)\left(\frac{\rho_g}{\rho_f}\right)^{2/3}\right]^{-1}, \tag{3}$$

or derived using the homogeneous equilibrium model,

$$\alpha = \left[1 + \left(\frac{1-x}{x}\right)\left(\frac{\rho_g}{\rho_f}\right)\right]^{-1}. \tag{4}$$

The gravitational pressure gradient is expressed as

$$-\left(\frac{dp}{dz}\right)_G = [\alpha\rho_g + (1-\alpha)\rho_f] g \sin\phi, \tag{5}$$

where ϕ is the channel's inclination angle and $-(dp/dz)_G = 0$ for horizontal flows. Unlike macro-channel flows, where gravitational effects can be significant, especially for low mass velocities, these effects are far less significant for mini/micro-channel flows, which are dominated by high velocities and large shear stresses.

The two-phase frictional pressure drop, $\Delta P_{tp,F}$, can be predicted according to either the homogeneous equilibrium model or semi-empirical correlations. Using the homogeneous equilibrium model, the two-phase frictional pressure gradient can be determined from [73]

$$-\left(\frac{dP}{dz}\right)_F = \frac{2f_{tp}\bar{\rho}u^2}{D_h} = \frac{2f_{tp}\upsilon_f G^2}{D_h}\left(1 + x\frac{\upsilon_{fg}}{\upsilon_f}\right), \tag{6}$$

where

$$f_{tp} = 16\,Re_{tp}^{-1} \text{ for } Re_{tp} < 2000, \tag{7a}$$

$$f_{tp} = 0.079\,Re_{tp}^{-0.25} \text{ for } 2000 \leqslant Re_{tp} < 20,000, \tag{7b}$$

and

$$f_{tp} = 0.046\,Re_{tp}^{-0.2} \text{ for } Re_{tp} \geqslant 20,000. \tag{7c}$$

Different predictions of $\Delta P_{tp,F}$ are possible, depending on which mixture viscosity model, Table 1, is used to calculate the two-phase Reynolds number, Re_{tp}, which is defined as GD_h/μ_{tp}.

Table 2 provides a summary of two-phase frictional pressure drop correlations that have been recommended previously for macro-channels [41–45] and mini/micro-channels [46–57] for adiabatic, condensing, and boiling flows. Most of these correlations are formulated in accordance with a Lockhart–Martinelli type [41] separated flow model, with the two-phase frictional pressure gradient expressed as the product of the frictional pressure gradient for each phase (based on actual flow rate for the individual phase) and a corresponding two-phase pressure drop multiplier.

Table 1
Two-phase mixture viscosity models employed in the homogeneous equilibrium model.

Author(s)	Equation
McAdams et al. [34]	$\frac{1}{\mu_{tp}} = \frac{x}{\mu_g} + \frac{1-x}{\mu_f}$
Akers et al. [35]	$\mu_{tp} = \frac{\mu_f}{\left[(1-x)+x\left(\frac{\upsilon_g}{\upsilon_f}\right)^{0.5}\right]}$
Cicchitti et al. [36]	$\mu_{tp} = x\mu_g + (1-x)\mu_f$
Owens [37]	$\mu_{tp} = \mu_f$
Dukler et al. [38]	$\mu_{tp} = \frac{x\upsilon_g\mu_g + (1-x)\upsilon_f\mu_f}{x\upsilon_g + (1-x)\upsilon_f}$
Beattie and Whalley [39]	$\mu_{tp} = \omega\mu_g + (1-\omega)(1+2.5\omega)\mu_f$ $\omega = \frac{x\upsilon_g}{\upsilon_f + x\upsilon_{fg}}$
Lin et al. [40]	$\mu_{tp} = \frac{\mu_f\mu_g}{\mu_g + x^{1.4}(\mu_f - \mu_g)}$

$$\left(\frac{dP}{dz}\right)_F = \left(\frac{dP}{dz}\right)_f \phi_f^2 = \left(\frac{dP}{dz}\right)_g \phi_g^2, \tag{8}$$

where

$$-\left(\frac{dP}{dz}\right)_f = \frac{2f_f\upsilon_f G^2(1-x)^2}{D_h} \tag{9a}$$

and

$$-\left(\frac{dP}{dz}\right)_g = \frac{2f_g\upsilon_g G^2 x^2}{D_h}. \tag{9b}$$

The friction factor for phase k (which denotes f for liquid or g for vapor) in Eqs. (9a) and (9b) is given by

$$f_k = 16\,Re_k^{-1} \text{ for } Re_k < 2000, \tag{10a}$$

$$f_k = 0.079\,Re_k^{-0.25} \text{ for } 2000 \leqslant Re_k < 20,000, \tag{10b}$$

$$f_k = 0.046\,Re_k^{-0.2} \text{ for } Re_k \geqslant 20,000, \tag{10c}$$

$$Re_k = Re_f = \frac{G(1-x)D_h}{\mu_f} \text{ for liquid}, \tag{11a}$$

and

$$Re_k = Re_g = \frac{GxD_h}{\mu_g} \text{ for vapor}. \tag{11b}$$

For laminar flow in rectangular channels, the two-phase friction factor can be obtained from [74]

$$f_k Re_k = 24(1 - 1.3553\beta + 1.9467\beta^2 - 1.7012\beta^3 + 0.9564\beta^4 - 0.2537\beta^5). \tag{12}$$

The correlations in Table 2 are used to determine the two-phase frictional pressure gradient. The two-phase pressure drop can be determined by integrating Eqs. (2), (5), (6), and (8) numerically according to

$$\Delta P_{tp} = \int_0^{L_{tp}} \left[-\left(\frac{dP}{dz}\right)_F - \left(\frac{dP}{dz}\right)_G - \left(\frac{dP}{dz}\right)_A\right] dz. \tag{13}$$

It should be emphasized that the correlations in Table 2 were derived for specific fluids and ranges of operating conditions. Notice that the macro-channel correlations are generally based on larger databases than correlations developed specifically for mini/micro-channel flows. For example, the popular macro-channel correlations of Friedel [42] and Müller-Steinhagen and Heck [43] are derived from two-phase frictional pressure drop databases consisting of 25,000 and 9300 data points, respectively. The correlation of Mishima and Hibiki [46], which is based on data for adiabatic air–water flow in 1–4 mm diameter circular tubes, has shown good predictions of mini/micro-channel pressure drop data for both adiabatic flows [15] and boiling flows [22,25]. The correlations of Li and Wu [55,57] are based on 769 adiabatic two-phase pressure drop data points for refrigerants, ammonia, propane, and nitrogen with hydraulic diameters from 0.148 to 3.25 mm.

Additionally, some correlations are recommended for specific laminar or turbulent flow states. For example, the correlation of Yang and Webb [47] is applicable only to turbulent flows ($Re_{fo} > 2500$), and the correlation of Hwang and Kim [53] for $Re_{fo} < 2000$. The correlation of Zhang et al. [56], which is a modified form of Mishima and Hibiki's [46], is not recommended for turbulent liquid-turbulent vapor flow.

3. New consolidated mini/micro-channel database

In the present study, a total of 2378 two-phase pressure drop data points for flow boiling in mini/micro-channels are amassed from 16 sources [18–33]. The database consists of 2033 single-channel data points from 12 sources, and 345 multi-channel data points from 4 sources.

Table 3 provides key information on the individual databases incorporated in the consolidated database. Notice that some of the data are purposely excluded from individual databases. These include enhanced (*e.g.,* micro-fin) tube data such as those of Monroe et al. [21], and oil mixture data such as those of Hu et al. [26]. The generalized correlation sought in this study concerns smooth surfaces, therefore, most of the data in the consolidated database are for surfaces with a relative roughness of 0.001–0.0001, except for the data by Ducoulombier [28] and Maqbool et al. [33], which have relative roughness values of 0.0015 and 0.0021, respectively. Also excluded are data points displaying strong departure from the majority of comparable data, such as those of Yan and Lin [48].

The consolidated database includes 1883 frictional pressure drop data points from 11 sources and 495 total pressure drop data points from 5 sources. The 1883 frictional pressure drop data were determined by the original authors by subtracting the accelerational component from the measured total pressure drop. As indicated in Eq. (2), calculating the acceleration pressure drop requires a relation for void fraction. Huo [23] used Lockhart and Martinelli's [41] void fraction relation,

$$\alpha = \left[1 + 0.28\left(\frac{1-x}{x}\right)^{0.64}\left(\frac{\rho_g}{\rho_f}\right)^{0.36}\left(\frac{\mu_f}{\mu_g}\right)^{0.07}\right]^{-1}, \tag{14}$$

Hu et al. [26], Quibén et al. [27], Ducoulombier [28], Tibiriçá and Ribatski [29] and Tibiriçá et al. [30] used Rouhani and Axelsson's [75] relation,

$$\alpha = \frac{x}{\rho_g}\left[\{1 + 0.12(1-x)\}\left(\frac{x}{\rho_g} + \frac{1-x}{\rho_f}\right) + \frac{1.18(1-x)\{g\sigma(\rho_f - \rho_f)\}^{0.25}}{G\rho_f^{0.5}}\right]^{-1}, \tag{15}$$

Maqbool et al. [33] used Woldesemayat and Ghajar's [76] relation,

$$\alpha = \frac{J_g}{J_g\left[1 + \left(\frac{J_f}{J_g}\right)\left(\frac{\rho_g}{\rho_f}\right)^{0.1}\right] + 2.9\left[\frac{gD_h\sigma(1+\cos\phi)(\rho_f - \rho_g)}{\rho_f^2}\right]^{0.25}(1.22 + 1.22\sin\phi)^{\frac{p_{atm}}{p}}}, \tag{16}$$

and Tran [19], Pettersen [20], and Owhaib et al. [25] used Zivi's [72] void fraction relation, Eq. (3). Wu et al. [31] neglected the accelerational pressure drop because of the short length of their test section.

As will be shown later in this study, using the void fraction relation derived from the homogeneous equilibrium model, Eq. (4),

Table 2
Two-phase frictional pressure gradient correlations.

Author(s)	Equation	Remarks
Lockhart and Martinelli [41]	$\left(\frac{dP}{dz}\right)_F = \left(\frac{dP}{dz}\right)_f \phi_f^2, \phi_f^2 = 1 + \frac{C}{X} + \frac{1}{X^2}, X^2 = \frac{(dP/dz)_f}{(dP/dz)_g}$ $C_{vv} = 5$, $C_{tv} = 10$, $C_{vt} = 12$, $C_{tt} = 20$	D_h = 1.49–25.83 mm, adiabatic, water, oils, hydrocarbons
Friedel [42]	$\left(\frac{dP}{dz}\right)_F = \left(\frac{dP}{dz}\right)_{fo} \phi_{fo}^2$ $\phi_{fo}^2 = (1-x)^2 + x^2\left(\frac{v_g}{v_f}\right)\left(\frac{f_{go}}{f_{fo}}\right) + 3.24x^{0.78}(1-x)^{0.224}\left(\frac{v_g}{v_f}\right)^{0.91}\left(\frac{\mu_g}{\mu_f}\right)^{0.19}\left(1-\frac{\mu_g}{\mu_f}\right)^{0.7} Fr_{tp}^{-0.045} We_{tp}^{-0.035}$ $Fr_{tp} = \frac{G^2}{gD_h\rho_H^2}, We_{tp} = \frac{G^2 D_h}{\sigma\rho_H}, \rho_H = \frac{1}{x v_g + (1-x)v_f}$	D > 4 mm, air–water, air-oil, R12 (25,000 data points)
Müller-Steinhagen and Heck [43]	$\left(\frac{dP}{dz}\right)_F = \left\{\left(\frac{dP}{dz}\right)_{fo} + 2\left[\left(\frac{dP}{dz}\right)_{go} - \left(\frac{dP}{dz}\right)_{fo}\right]x\right\}(1-x)^{1/3} + \left(\frac{dP}{dz}\right)_{go} x^3$	D = 4–392 mm, air–water, water, hydrocarbons, refrigerants (9300 data points)
Jung and Radermacher [44]	$\left(\frac{dP}{dz}\right)_F = \left(\frac{dP}{dz}\right)_{fo} \phi_{fo}^2, \phi_{fo}^2 = 12.82 X_{tt}^{-1.47}(1-x)^{1.8},$ $X_{tt} = \left(\frac{\mu_f}{\mu_g}\right)^{0.1}\left(\frac{1-x}{x}\right)^{0.9}\left(\frac{\rho_g}{\rho_f}\right)^{0.5}$	D = 9.1 mm, annular flow boiling, pure and mixed refrigerants
Wang et al. [45]	For $G \geqslant 200$ kg/m^{2}s, $\left(\frac{dP}{dz}\right)_F = \left(\frac{dP}{dz}\right)_g \phi_g^2, \phi_g^2 = 1 + 9.4X^{0.62} + 0.564X^{2.45}$ For G < 200 kg/m^{2}s, $\left(\frac{dP}{dz}\right)_F = \left(\frac{dP}{dz}\right)_f \phi_f^2, \phi_f^2 = 1 + \frac{C}{X} + \frac{1}{X^2},$ $C = 4.566 \times 10^{-6} X^{0.128} Re_{fo}^{0.938}\left(\frac{v_f}{v_g}\right)^{2.15}\left(\frac{\mu_f}{\mu_g}\right)^{5.1}$	D = 6.5 mm, adiabatic, R22, R134a, R407C
Mishima and Hibiki [46]	$\left(\frac{dP}{dz}\right)_F = \left(\frac{dP}{dz}\right)_f \phi_f^2, \phi_f^2 = 1 + \frac{C}{X} + \frac{1}{X^2}$ For rectangular channel, $C = 21\,[1 - \exp(-0.319 D_h)]$; D_h(mm) For circular tube, $C = 21[1 - \exp(-0.333D)]$; D(mm)	D = 1.05–4.08 mm, adiabatic, air–water
Yang and Webb [47]	$\left(\frac{dP}{dz}\right)_F = -0.87 Re_{eq}^{0.12} f_{fo} \frac{G_{eq}^2 v_f}{D_h}, Re_{eq} = \frac{G_{eq} D_h}{\mu_f}, G_{eq} = G\left[(1-x) + x\left(\frac{\rho_f}{\rho_g}\right)^{0.5}\right]$	D_h = 1.56, 2.64 mm, adiabatic, R12, Re_{fo} > 2500
Yan and Lin [48]	$\left(\frac{dP}{dz}\right)_F = -0.22 Re_{eq}^{-0.1} \frac{G_{eq}^2 v_f}{D_h}$	D = 2.0 mm, boiling, R134a
Tran et al. [49]	$\left(\frac{dP}{dz}\right)_F = \left(\frac{dP}{dz}\right)_{fo} \phi_{fo}^2, N_{conf} = \sqrt{\frac{\sigma}{g(\rho_f - \rho_g)D_h^2}}\left(= \sqrt{\frac{1}{Bd}}\right)$ $\phi_{fo}^2 = 1 + \left[4.3\frac{(dP/dz)_{go}}{(dP/dz)_{fo}} - 1\right][N_{conf} x^{0.875}(1-x)^{0.875} + x^{1.75}]$	D_h = 2.40–2.92 mm, boiling, refrigerants
Chen et al. [50]	$\left(\frac{dP}{dz}\right)_F = \left(\frac{dP}{dz}\right)_{fo,Friedel} \Omega, Bd^* = g(\rho_f - \rho_g)\frac{(D_h/2)^2}{\sigma}$ For $Bd^* < 2.5$, $\Omega = \frac{0.0333 Re_{fo}^{0.45}}{Re_g^{0.09}(1+0.4e^{-Bd^*})}$ For $Bd^* \geqslant 2.5$, $\Omega = \frac{We_{fo}^{0.2}}{(2.5+0.06Bd^*)}$	D = 1.02–9 mm, adiabatic, air–water, R410A, ammonia
Lee and Lee [51]	$\left(\frac{dP}{dz}\right)_F = \left(\frac{dP}{dz}\right)_f \phi_f^2, \phi_f^2 = 1 + \frac{C}{X} + \frac{1}{X^2}, \psi = \frac{\mu_f j_f}{\sigma}, \lambda = \frac{\mu_f^2}{\rho_f \sigma D_h}$ $C_{vv} = 6.833 \times 10^{-8} \lambda^{-1.317} \psi^{0.719} Re_{fo}^{0.557}, C_{tv} = 3.627 Re_{fo}^{0.174}$ $C_{vt} = 6.185 \times 10^{-2} Re_{fo}^{0.726}, C_{tt} = 0.048 Re_{fo}^{0.451}$	D_h = 0.78–6.67 mm, adiabatic, air–water
Yu et al. [52]	$\left(\frac{dP}{dz}\right)_F = \left(\frac{dP}{dz}\right)_f \phi_f^2, \phi_f^2 = \left[18.65\left(\frac{v_f}{v_g}\right)^{0.5}\left(\frac{1-x}{x}\right)\frac{Re_g^{0.1}}{Re_f^{0.5}}\right]^{-1.9}$	D = 2.98 mm, boiling, water
Hwang and Kim [53]	$\left(\frac{dP}{dz}\right)_F = \left(\frac{dP}{dz}\right)_f \phi_f^2, \phi_f^2 = 1 + \frac{C}{X} + \frac{1}{X^2}, C = 0.227 Re_{fo}^{0.452} X^{-0.32} N_{conf}^{-0.82}$	D = 0.244, 0.430, 0.792 mm, adiabatic, R134a, Re_{fo} < 2000
Sun and Mishima [54]	For Re_f < 2000 and Re_g < 2000, $\left(\frac{dP}{dz}\right)_F = \left(\frac{dP}{dz}\right)_f \phi_f^2, \phi_f^2 = 1 + \frac{C}{X} + \frac{1}{X^2},$ $C = 26\left(1 + \frac{Re_f}{1000}\right)\left[1 - \exp\left(\frac{-0.153}{0.27N_{conf}+0.8}\right)\right]$ For $Re_f \geqslant 2000$ or $Re_g \geqslant 2000$, $\left(\frac{dP}{dz}\right)_F = \left(\frac{dP}{dz}\right)_f \phi_f^2, \phi_f^2 = 1 + \frac{C}{X^{1.19}} + \frac{1}{X^2}, C = 1.79\left(\frac{Re_g}{Re_f}\right)^{0.4}\left(\frac{1-x}{x}\right)^{0.5}$	D_h = 0.506–12 mm, air–water, refrigerants, CO_2 (2092 data points)
Li and Wu [55]	$\left(\frac{dP}{dz}\right)_F = \left(\frac{dP}{dz}\right)_f \phi_f^2, \phi_f^2 = 1 + \frac{C}{X} + \frac{1}{X^2}, Bd = \frac{g(\rho_f - \rho_g)D_h^2}{\sigma}$ For $Bd \leqslant 1.5$, $C = 11.9 Bd^{0.45}$ For $1.5 < Bd \leqslant 11$, $C = 109.4(Bd\,Re_f^{0.5})^{-0.56}$ For Bd > 11, Beattie and Whalley (1982) correlation is recommended	D_h = 0.148–3.25 mm, adiabatic, refrigerants, ammonia, propane, nitrogen (769 data points)
Zhang et al. [56]	$\left(\frac{dP}{dz}\right)_F = \left(\frac{dP}{dz}\right)_f \phi_f^2, \phi_f^2 = 1 + \frac{C}{X} + \frac{1}{X^2}, C = 21[1 - \exp(-0.142/N_{conf})]$	D_h = 0.07–6.25 mm, adiabatic, air/N_2-water, air/ethanol, refrigerants, ammonia, water (2201 data points), not recommended for turbulent liquid-turbulent vapor (tt) flow
Li and Wu [57]	For Bd < 0.1, $\left(\frac{dP}{dz}\right)_F = \left(\frac{dP}{dz}\right)_f \phi_f^2, \phi_f^2 = 1 + \frac{C}{X} + \frac{1}{X^2}, C = 5.60 Bd^{0.28}$ For $Bd \geqslant 0.1$ and $Bd Re_f^{0.5} \leqslant 200$, $\left(\frac{dP}{dz}\right)_F = \left(\frac{dP}{dz}\right)_{fo} \phi_{fo}^2, \phi_{fo}^2 = (1-x)^2 + 2.87x^2 P_R^{-1} + 1.54 Bd^{0.19}\left(\frac{\rho_f - \rho_g}{\rho_H}\right)^{0.81}$ For $Bd Re_f^{0.5} > 200$, Beattie and Whalley (1982) correlation is recommended	Same data as Li and Wu [55]

Table 3
Two-phase frictional pressure drop data for mini/micro-channel boiling flows included in the consolidated database.

Author(s)	Channel geometry*	Channel material	D_h (mm)	Fluid(s)	G (kg/m^{2}s)	Data type	Data points
Lezzi et al. [18]	C single, H	Stainless steel	1.0	Water	776–2738	ΔP_{tp}	86
Tran [19]	C single, H	Brass	2.46	R12, R134a	33–832	$\Delta P_{tp,F}$	439
Pettersen [20]	C multi, H	Aluminum	0.81	CO_2	190–570	$\Delta P_{tp,F}$	57
Monroe et al. [21]	R multi, H	Aluminum	1.66	R134a	99–402	ΔP_{tp}	37
Qu and Mudawar [22]	R multi, H	Copper + Lexan cover	0.349	Water	135–402	ΔP_{tp}	164
Huo [23]	C single, VU	Stainless steel	2.01, 4.26	R134a	400–500	$\Delta P_{tp,F}$	74
Lee and Mudawar [24]	R multi, H	Copper + Lexan cover	0.349	R134a	128–657	ΔP_{tp}	87
Owhaib et al. [25]	C single, VU	Stainless steel	0.826, 1.224, 1.7	R134a	100–400	$\Delta P_{tp,F}$	53
Hu et al. [26]	C single, H	–	2.0, 4.18	R410A	200–620	$\Delta P_{tp,F}$	48
Quibén et al. [27]	R single, H	Copper	3.5, 3.71, 4.88, 5.35	R22, R410A	150–500	$\Delta P_{tp,F}$	264
Ducoulombier [28]	C single, H	Stainless steel	0.529	CO_2	400–1200	$\Delta P_{tp,F}$	268
Tibiriçá and Ribatski [29]	C single, H	Stainless steel	2.32	R245fa	199–701	$\Delta P_{tp,F}$	142
Tibiriçá et al. [30]	C single, H	Stainless steel	2.32	R134a	100–600	$\Delta P_{tp,F}$	49
Wu et al. [31]	C single, H	Stainless steel	1.42	CO_2	300–600	$\Delta P_{tp,F}$	254
Kharangate et al. [32]	R single, H/VU	Copper bottom + Lexan	3.33	FC72	177–1652	ΔP_{tp}	121
Maqbool et al. [33]	C single, VU	Stainless steel	1.224, 1.70	Ammonia	100–500	$\Delta P_{tp,F}$	235
Total							2378

* C: circular, R: rectangular, H: horizontal, VU: vertical upward.

generally overpredicts experimental data compared to other void fraction relations. Therefore, any frictional pressure drop data points from original sources that are determined by subtracting the accelerational pressure drop from the measured total pressure drop using the homogeneous void fraction relation are excluded from the consolidated database. For the total pressure drop data points, the frictional pressure gradient in the present study is isolated by subtracting the accelerational pressure gradient determined using Eq. (2) and Zivi's [72] void fraction relation, Eq. (3). Notice that acceleration can contribute an appreciable fraction of total pressure drop, especially in high-flux micro-channel boiling flows corresponding to large axial quality gradients. The effect of using different void fraction models to determine the accelerational pressure drop will be discussed later.

Unlike prior databases that have been used to correlate frictional pressure drop in mini/micro-channels, the present consolidated database includes a broad range of reduced pressures, 0.005 to 0.78. The high pressure data include those of Pettersen [20], P_R = 0.47–0.78, Ducoulombier [28], P_R = 0.36–0.47, and Wu et al. [31], 0.14–0.47.

Overall, the new consolidated database consists of 2378 pressure drop data points with the following coverage:

- Working fluid: R12, R134a, R22, R245fa, R410A, FC-72, ammonia, CO_2, and water
- Hydraulic diameter: $0.349 < D_h < 5.35$ mm
- Mass velocity: $33 < G < 2738$ kg/m^{2}s
- Liquid-only Reynolds number: $156 < Re_{fo} = GD_h/\mu_f < 28{,}010$
- Superficial liquid Reynolds number: $0 < Re_f = G(1-x)D_h/\mu_f < 16{,}020$
- Superficial vapor Reynolds number: $0 < Re_g = GxD_h/\mu_g < 199{,}500$
- Flow quality: $0 < x < 1$
- Reduced pressure: $0.005 < P_R < 0.78$.

4. Evaluation of previous correlations

When comparing the consolidated database to the predictions of previous models or correlations, the thermophysical properties for different fluids are obtained using NIST's REFPROP 8.0 software [77], excepting those for FC-72, which are obtained from 3M Company. Table 4 provides representative values of the thermophysical properties of FC-72 over the ranges of interest. Three different parameters are used to assess the accuracy of individual models or correlations. θ and ξ are defined as the percentages of data points predicted within ±30% and ±50%, respectively, and MAE the mean absolute error, which is determined according to

$$\mathrm{MAE} = \frac{1}{N}\sum \frac{\left|dP/dz_{\mathrm{F,pred}} - dP/dz_{\mathrm{F,exp}}\right|}{dP/dz_{\mathrm{F},exp}} \times 100\%. \quad (17)$$

Figs. 2–4 compare the 2378 frictional pressure gradient data points for mini/micro-channel flow boiling with predictions of previous homogeneous equilibrium models [34–40], semi-empirical correlations for macro-channels [41–45], and semi-empirical correlations for mini/micro-channels [46–57], respectively. In each figure, the percentage MAE is indicated as λ, with λ_{vv}, λ_{vt}, λ_{tv} and λ_{tt} indicating MAE values for the laminar liquid-laminar vapor (*vv*), laminar liquid-turbulent vapor (*vt*), turbulent liquid-laminar vapor (*tv*), and turbulent liquid-turbulent vapor (*tt*) regimes, respectively.

In a recent study of the authors [71] concerning the development of a universal correlation for pressure drop in condensing and adiabatic mini/micro-channel flows, using the the homogeneous equilibrium model in conjunction with the viscosity models of McAdams et al. [34], Akers et al. [35], Cicchitti et al. [36], Owens [37], and Lin et al. [40] highly overpredicted data in the laminar-laminar (*vv*) regime, while most of the models showed fair predictions for the other flow regimes (*vt*, *tv*, *tt*), excepting those of Cicchitti et al. [36] and Owens [37], which highly overpredicted some of the data in the laminar-turbulent (*vt*) regime. For the present flow boiling pressure drop data, similar trends are observed for the laminar-laminar (*vv*) regime. As shown in Fig. 2, the viscosity models of McAdams et al., Akers et al., Cicchitti et al., Owens, and Lin et al. highly overpredict the flow boiling pressure drop data in the laminar-laminar (*vv*) regime. However, all of the models [34–40] (especially those of McAdams et al. [34], Dukler et al. [38], Beattie and Whalley [39], and Lin et al. [40]) underpredict the data in the other flow regimes (*vt*, *tv*, *tt*). The difference in predictive accuracy between condensing and adiabatic mini/micro-channel flows [71] on one hand and mini/micro-channel boiling flows, Fig. 2, on the other highlight the aforementioned

Table 4
Thermophysical properties of saturated FC-72.

T_{sat} (°C)	P_{sat} (kPa)	ρ_f (kg/m^3)	ρ_g (kg/m^3)	h_f (kJ/kg)	h_{fg} (kJ/kg)	μ_f (kg/m s)	σ (mN/m)
68	146.12	1562.5	19.03	108.77	91.00	3.85×10^{-4}	7.2351
72	164.89	1552.1	21.40	113.34	89.61	3.71×10^{-4}	6.8436
76	185.51	1541.6	24.01	117.95	88.20	3.57×10^{-4}	6.4522

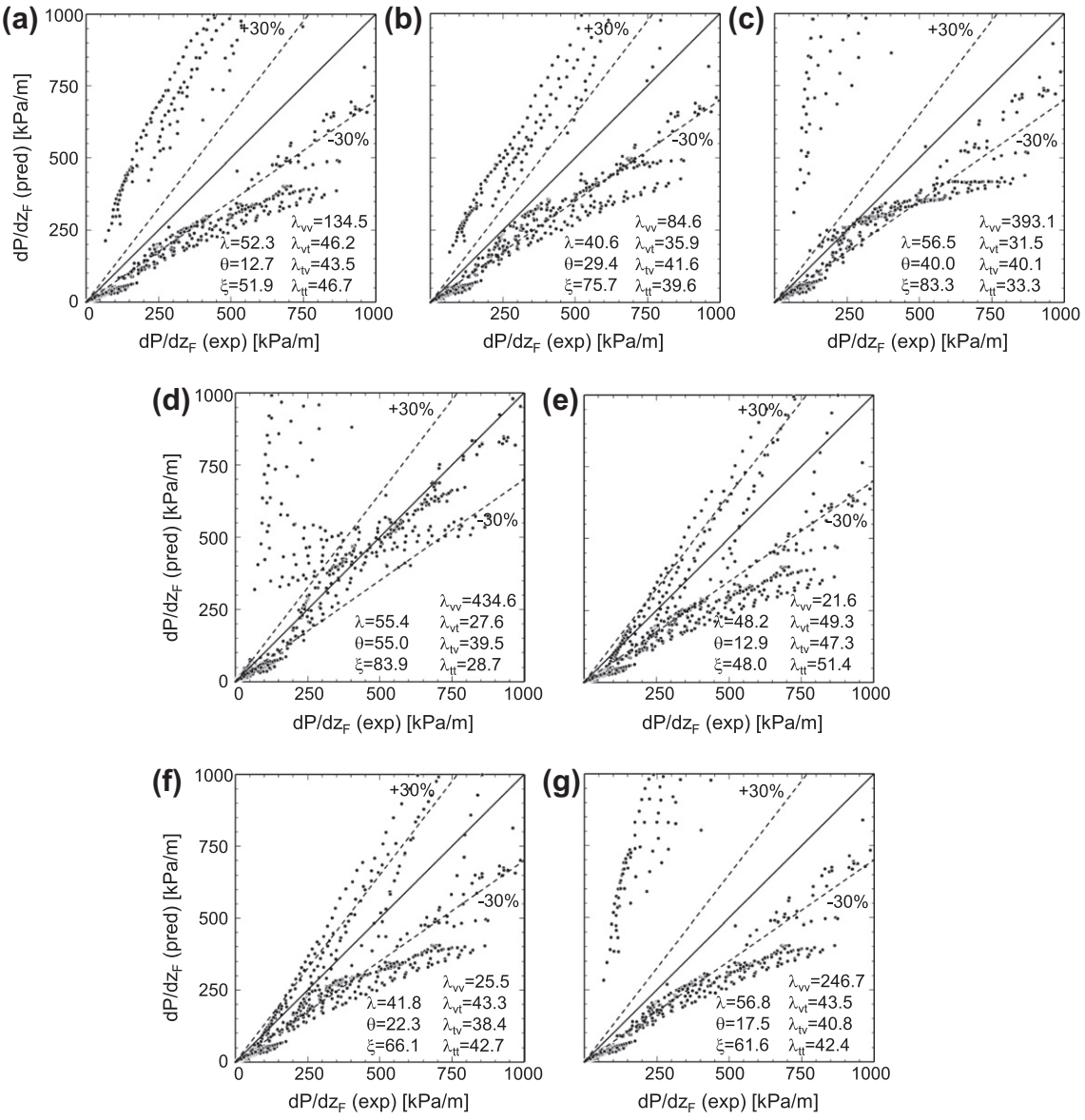

Fig. 2. Comparison of 2378 experimental data points with predictions of homogeneous equilibrium model using viscosity models of: (a) McAdams et al. [34], (b) Akers et al. [35], (c) Cicchitti et al. [36], (d) Owens [37], (e) Dukler et al. [38], (f) Beattie and Whalley [39], and (g) Lin et al. [40].

fundamental differences in flow structure, especially in regards to droplet entrainment. Droplet entrainment effects appear to be more significant at high mass velocities and turbulent flows than laminar flow, which is evidenced by the flow boiling data being underpredicted by the models in the *vt*, *tv*, and *tt* regimes, while the condensing and adiabatic data are predicted with fair accuracy for the same regimes.

Fig. 3 shows the frictional pressure gradient correlations recommended for macro-channels provide poor predictions for most of the consolidated database. The correlation of Lockhart and Martinelli [41] overpredicts the data in general, especially for the tt regime, while those of Friedel [42], Müller-Steinhagen and Heck [43], Jung and Radermacher [44], and Wang et al. [45] highly overpredict the data in the vv regime. Excluding the vv regime, the correlations of Friedel, and Müller-Steinhagen and Heck provide fair predictions, married by some scatter and underprediction by the latter. It is interesting to note that most data with diameters below 1 mm are overpredicted by Jung and Radermacher and Wang et al., which are intended for macro-channels.

As shown in Fig. 4, frictional pressure gradient correlations intended for mini/micro-channels show large scatter against most of the consolidated database. Notice that for the correlations of Yang and Webb [47], Hwang and Kim [53], and Zhang et al. [56], only the pressure gradient data corresponding to their validity range are considered. The correlations of Yan and Lin [48], Tran et al. [49], Chen et al. [50], Lee and Lee [51], and Yu et al. [52] show significant scatter; with significant overprediction of most of the data by Yan and Lin and Tran et al., and significant underprediction by Chen et al. and Yu et al. Most of the consolidated database is underpredicted by Hwang and Kim [53], Sun and Mishima [54], and Li and Wu [55,57], while micro-channel data with diameters smaller than 1 mm are predicted by Li and Wu with fair accuracy.

Among all previous models and correlations in Figs. 2–4, the correlation of Mishima and Hibiki [46] provides the best predictions, evidenced by a MAE of 27.6%, although this correlation underpredicts the data corresponding to $dP/dz_F > 10$ kPa/m, and overpredicts the data corresponding to $dP/dz_F < 10$ kPa/m. Interestingly, the correlation by Zhang et al., which is a modified form of

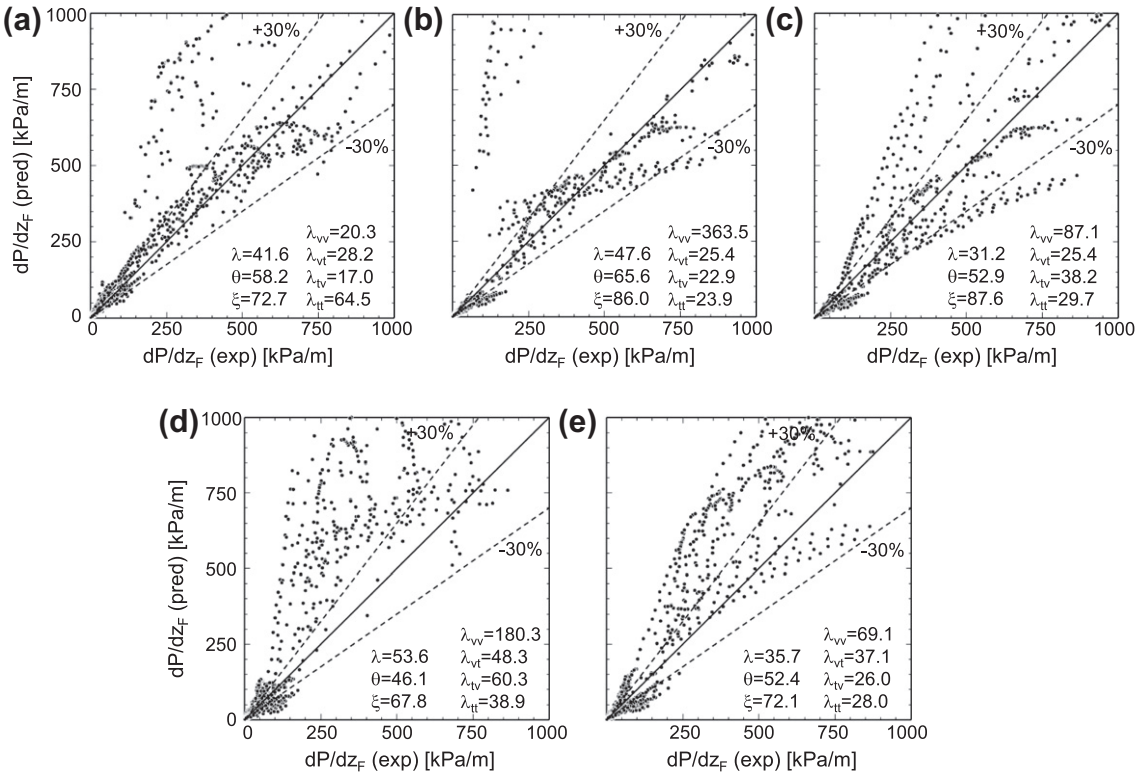

Fig. 3. Comparison of 2378 experimental data points with predictions of semi-empirical correlations recommended for macro-channels: (a) Lockhart and Martinelli [41], (b) Friedel [42], (c) Müller-Steinhagen and Heck [43], (d) Jung and Radermacher [44], and (e) Wang et al. [45].

the Mishima and Hibiki's correlation, underpredicts most of the consolidated database by a large margin.

5. New predictive two-phase pressure drop method

Using the original formulation of Lockhart and Martinelli [41], Kim and Mudawar [71] proposed a universal approach to predicting two-phase frictional pressure gradient for condensing and adiabatic mini/micro-channel flows, replacing the constant C in the Lockhart–Martinelli parameter with a function of dimensionless groups from Table 5 that capture the influence of small channel size. The pressure drop predictions in [71] were validated against a consolidated database consisting of 7115 frictional pressure drop data points from 36 sources. Fig. 5 shows the pressure drop correlation from [71] provides excellent predictions for all three separate subsets of the consolidated database: adiabatic liquid–gas flow, adiabatic liquid–vapor flow, and condensing flow, evidenced by MAE values of 25.7%, 23.7%, and 17.5%, respectively. The pressure gradient correlations for adiabatic liquid–gas, adiabatic liquid–vapor, and condensing flows (denoted as *non-boiling* flows hereafter) from [71] are provided in Table 5, where function C in the Lockhart–Martinelli correlation is denoted as $C_{non\text{-}boiling}$.

As discussed earlier, the previous models and correlations show a consistently different trend in predicting non-boiling mini/micro-channel data [71] versus the present consolidate database for mini/micro-channel flow boiling. Moderate or sometimes significant underprediction of the present consolidated flow boiling database is observed compared to the non-boiling data. Most notably, the homogeneous equilibrium viscosity models by Dukler et al. [38] and Beattie and Whalley [39], and the correlation by Müller-Steinhagen and Heck [43] underpredict the present flow boiling database, despite their good predictions of the non-boiling data. Deviations in the prediction of flow boiling versus non-boiling data when using the same model or correlation is intensified with increasing heat flux. To compensate for this deviation, the C function in the Lockhart–Martinelli parameter is modified by the Weber and Boiling numbers, which are defined, respectively, as

$$We_{fo} = \frac{G^2 D_h}{\rho_f \sigma}, \tag{18}$$

and

$$Bo = \frac{q''_H}{Gh_{fg}}, \tag{19}$$

where q''_H is the effective heat flux averaged over the heated perimeter of the channel. The ratio of the flow channel's heated to wetted perimeters, P_H/P_F, is also considered to cope with three-sided wall heating [22,24] as well as one-sided wall heating [32]. Using the entire consolidated database for flow boiling, the following correlations for the C function are derived based on their ability to yield the least MAE values for two different ranges of Re_f, turbulent and laminar,

$$C = C_{non\text{-}boiling}\left[1 + 60We_{fo}^{0.32}\left(Bo\frac{P_H}{P_F}\right)^{0.78}\right] \quad \text{for } Re_f \geqslant 2000, \tag{20a}$$

and

$$C = C_{non\text{-}boiling}\left[1 + 530We_{fo}^{0.52}\left(Bo\frac{P_H}{P_F}\right)^{1.09}\right] \quad \text{for } Re_f < 2000, \tag{20b}$$

respectively.

Fig. 6 shows the new two-phase frictional pressure gradient correlation for flow boiling, which is summarized in Table 5, predicts the entire 2378 consolidated mini/micro-channel flow boiling database quite accurately, with MAE values of 13.7%, 18.1%, 22.6%,

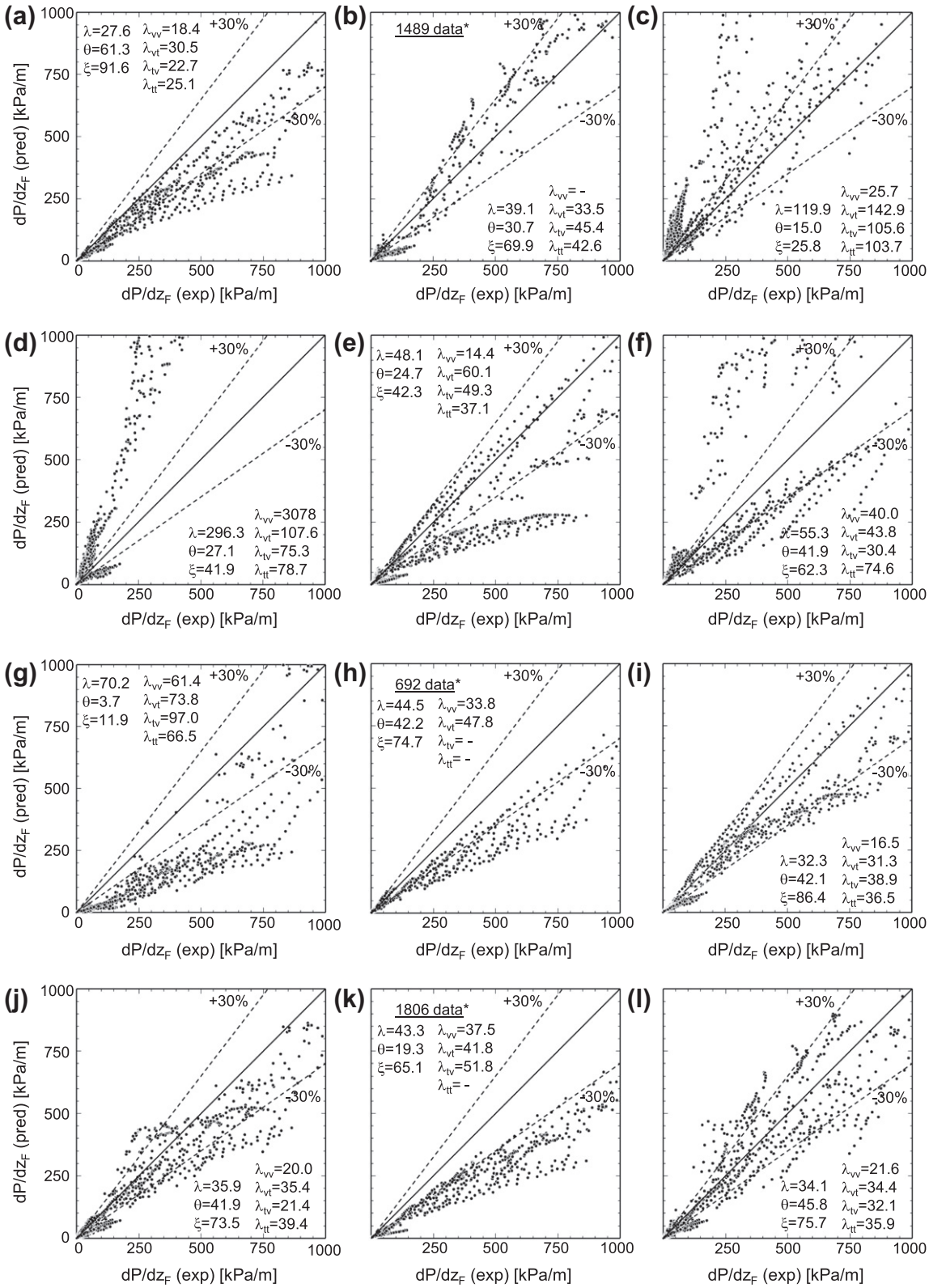

Fig. 4. Comparison of 2378 experimental data points with predictions of semi-empirical correlations recommended for mini/micro-channels: (a) Mishima and Hibiki [46], (b) Yang and Webb [47], (c) Yan and Lin [48], (d) Tran et al. [49], (e) Chen et al. [50], (f) Lee and Lee [51], (g) Yu et al. [52], (h) Hwang and Kim [53], (i) Sun and Mishima [54], (j) Li and Wu [55], (k) Zhang et al. [56], and (l) Li and Wu [57]. Data marked (∗) correspond to Re_{fo} > 2500 for Yang and Webb, Re_{fo} < 2000 for Hwang and Kim, and exclude turbulent liquid-turbulent vapor (*tt*) for Zhang et al..

and 16.4% for the laminar-laminar (*vv*), laminar-turbulent (*vt*), turbulent-laminar (*tv*), turbulent-turbulent (*tt*) flow regimes, respectively.

Achieving low overall MAE values is by no means the only definitive means for ascertaining the effectiveness of the new predictive approach. It is also crucial that the correlation is evenly

Table 5
New boiling pressure drop correlation for flow boiling in mini/micro-channels in both single- and multi-channel configurations. The non-boiling pressure drop correlations for adiabatic and condensing flows are based on Ref. [71].

$\left(\frac{dP}{dz}\right)_F = \left(\frac{dP}{dz}\right)_f \phi_f^2$

where $\phi_f^2 = 1 + \frac{C}{X} + \frac{1}{X^2}, X^2 = \frac{(dP/dz)_f}{(dP/dz)_g}$

$-\left(\frac{dP}{dz}\right)_f = \frac{2f_f v_f G^2 (1-x)^2}{D_h}, -\left(\frac{dP}{dz}\right)_g = \frac{2f_g v_g G^2 x^2}{D_h}$

$f_k = 16 Re_k^{-1}$ for $Re_k < 2000$

$f_k = 0.079 Re_k^{-0.25}$ for $2000 \leqslant Re_k < 20,000$

$f_k = 0.046 Re_k^{-0.2}$ for $Re_k \geqslant 20,000$

for laminar flow in rectangular channel,

$f_k Re_k = 24(1 - 1.3553\beta + 1.9467\beta^2 - 1.7012\beta^3 + 0.9564\beta^4 - 0.2537\beta^5)$

where subscript k denotes f or g for liquid and vapor phases, respectively,

$Re_f = \frac{G(1-x)D_h}{\mu_f}, Re_g = \frac{GxD_h}{\mu_g}, Re_{fo} = \frac{GD_h}{\mu_f}, Su_{go} = \frac{\rho_g \sigma D_h}{\mu_g^2}, We_{fo} = \frac{G^2 D_h}{\rho_f \sigma}, Bo = \frac{q''_H}{Gh_{fg}}$

	$C_{non\text{-}boiling}$
$Re_f \geqslant 2000, Re_g \geqslant 2000$ (tt)	$0.39 Re_{fo}^{0.03} Su_{go}^{0.10} \left(\frac{\rho_f}{\rho_g}\right)^{0.35}$
$Re_f \geqslant 2000, Re_g < 2000$ (tv)	$8.7 \times 10^{-4} Re_{fo}^{0.17} Su_{go}^{0.50} (\frac{\rho_f}{\rho_g})^{0.14}$
$Re_f < 2000, Re_g \geqslant 2000$ (vt)	$0.0015 Re_{fo}^{0.59} Su_{go}^{0.19} (\frac{\rho_f}{\rho_g})^{0.36}$
$Re_f < 2000, Re_g < 2000$ (vv)	$3.5 \times 10^{-5} Re_{fo}^{0.44} Su_{go}^{0.50} (\frac{\rho_f}{\rho_g})^{0.48}$
	C
$Re_f \geqslant 2000$	$C_{non\text{-}boiling}[1 + 60 We_{fo}^{0.32} (Bo \frac{P_H}{P_F})^{0.78}]$
$Re_f < 2000$	$C_{non\text{-}boiling}[1 + 530 We_{fo}^{0.52} (Bo \frac{P_H}{P_F})^{1.09}]$

successful at predicting data over relatively broad ranges of all relevant parameters [69–71].

Fig. 7 shows, for each parameter, both a lower bar chart distribution of number of data points, and corresponding upper bar chart distribution of MAE in the predictions of the new correlation. The distributions of the entire 2378-point database are examined relative to working fluid, hydraulic diameter, D_h, mass velocity, G, liquid-only Reynolds number, Re_{fo}, quality, x, and reduced pressure, P_R. Overall, the new correlation shows very good predictions for most parameter bins, evidenced by MAE values mostly below 20%.

Another equally crucial measure of the predictive accuracy of the correlation is the ability to provide evenly good predictions for individual databases comprising the consolidated database. Table 6 compares individual databases from 16 sources with predictions of the present correlation as well as select previous correlations that have shown relatively superior predictive capability as discussed earlier. Unlike the non-boiling data discussed in [71], all the viscosity models used in conjunction with the homogeneous equilibrium model show poor predictions of the present flow boiling data. Of the previous predictive tools, only the correlation of Mishima and Hibiki [46] shows fair accuracy in predicting the consolidated data, although it underpredicts diameters below 1 mm. Table 6 shows the new correlation provides excellent predictions for all individual databases, with 9 databases predicted more accurately than any of the previous models or correlations, and the best overall MAE of 17.2%. The accuracy and limitations of previous correlations are assessed by comparing predictions over the entire range of hydraulic diameters as shown in Fig. 8. Notice how the correlations intended for macro-channels (Friedel [42], Müller-Steinhagen and Heck [43], Wang et al. [45]) provide poor predictions for most diameters below 1 mm. The correlation of Li and Wu [57], which is based on D_h = 0.148–3.25 mm, provides acceptable predictions only diameters below 2 mm. In contrast, the new correlation shows good predictions over the entire range of diameters.

Fig. 9(a) and (b) show predictions of the new correlation technique compared to two subsets of the consolidated database: multi-channel flow and flow in single channels, respectively. The MAE for the 345 multi-channel data subset is 18.1%, with 89.6% and 97.4% of the data falling within ±30% and ±50% error bands, respectively. The corresponding values for the 2033 single-channel data subset are MAE of 17.1%, and 85.3% and 97.3% of the data falling within ±30% and ±50% error bands, respectively. The overall MAE based on the entire 2378 point database is 17.2%, with 85.9% and 97.4% of the data falling within ±30% and ±50% error bands, respectively.

One concern in using any two-phase pressure drop model or correlation is the determination of thermophysical properties. While many predictive methods require accounting for property variations along the flow channel, end users often prefer to use constant properties to simplify calculations. These two different approaches to predicting the frictional pressure gradient are compared using the new correlation technique. Fig. 10(a) and (b) compare 495 total pressure drop data points to predictions of the new correlation technique, with the thermophysical properties based on the average saturation temperature between the channel's inlet and outlet, and with the saturation temperature varying along the channel, respectively. To isolate the frictional pressure gradient from the experimental data, the accelerational pressure gradient is determined using Eq. (2) and Zivi's [72] void fraction relation, Eq. (3). Despite appreciable pressure changes between the channel inlet and outlet for high-flux data, Fig. 10(a) and (b) show the two different property calculation methods yield very close results. The predictive differences between the two methods are quite small: 1.08%, 0.21%, 0.38%, 0.09%, and 0.45% for the data of Lezzi et al. [18], Monroe et al. [21], Qu and Mudawar [22], Lee and Mudawar [24], and Kharangate et al. [32], respectively. Therefore, all calculations presented in this study are based on mean thermophysical properties unless indicated otherwise.

Table 7 compares the 495 total pressure drop data points [18,21,22,24,32] with the predictions of the new frictional pressure drop correlations, but with the accelerational pressure gradient determined using different void fraction models. Despite the appreciable axial changes in quality between the channel inlet and outlet, Table 7 shows that using the different void fraction relations of Lockhart and Martinelli [41], Zivi [72], Baroczy [78], Rouhani and Axelsson [75], and Woldesemayat and Ghajar [76] provides fairly similar results, evidenced by MAE values of 15.5%, 15.7%, 15.8%, 15.1%, and 16.3%, respectively. However, the void fraction relation derived from the homogeneous equilibrium

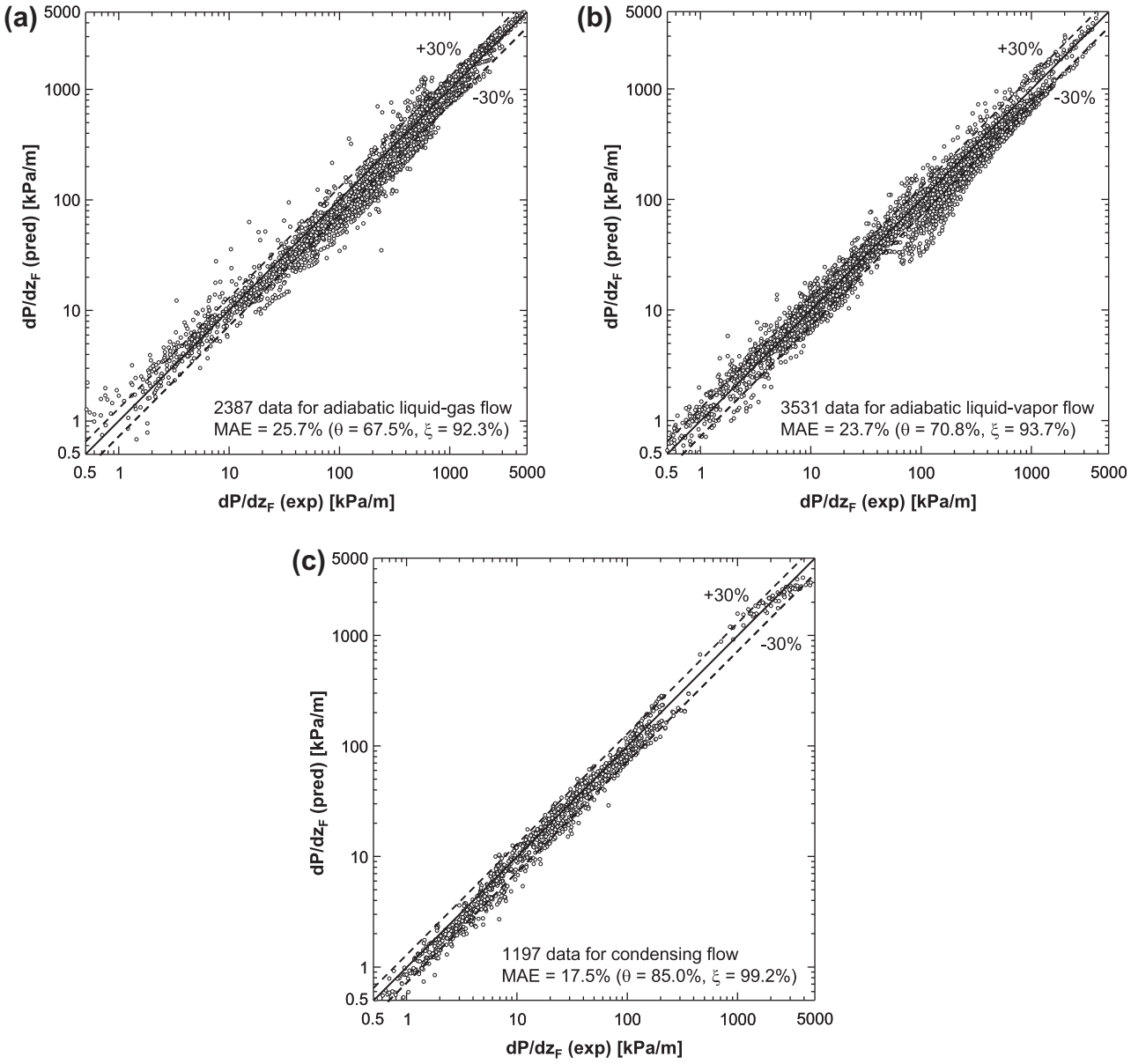

Fig. 5. Comparison of predictions of Kim and Mudawar's [71] correlation with three subsets of the consolidated database [71] corresponding to: (a) adiabatic liquid–gas flow, (b) adiabatic liquid–vapor flow, and (c) condensing flow.

model, Eq. (4), overpredicts the experimental data with a MAE of 49.6%, which is appreciably higher than those of the other void fraction relations. It can therefore be concluded that, in situations involving appreciable axial quality changes, the choice of void fraction relation in determining the accelerational pressure gradient (excluding the homogeneous equilibrium model) is relatively insignificant compared to the choice of frictional gradient correlation.

Despite the success of the present correlation technique in predicting the two-phase frictional gradient for mini/micro-channels, it is crucial that future studies pursue theoretical models that accurately capture interfacial interactions in small diameter channels. Because of drastic differences in interfacial behavior among different flow regimes, different models must be customized to tackle the specifics of the flow regime in question. For example, models for the annular regime must address the important influences of interfacial waves. As indicated in [71], past studies at PU-BTPFL involving adiabatic, heated and evaporating liquid films have shown that waves can have a profound influence on mass, momentum and heat transfer in the film [15,79–85]. Another important concern is accurate modeling of the dampening of turbulence near the vapor–liquid interface due to surface tension forces [66,86]. The advancement of modeling efforts can also benefit greatly from the use of sophisticated diagnostic techniques for measurement of annular film thickness and interfacial waves [85,87], albeit for small channel diameters. Models must also be developed that capture the transitions from bubbly to slug flow, and from slug to annular flow. Such models will play a major role in the development of new predictive techniques for both pressure drop and heat transfer coefficient for the individual flow regimes.

6. Conclusions

This study resulted in the development of a universal technique to predicting the two-phase frictional pressure gradient for

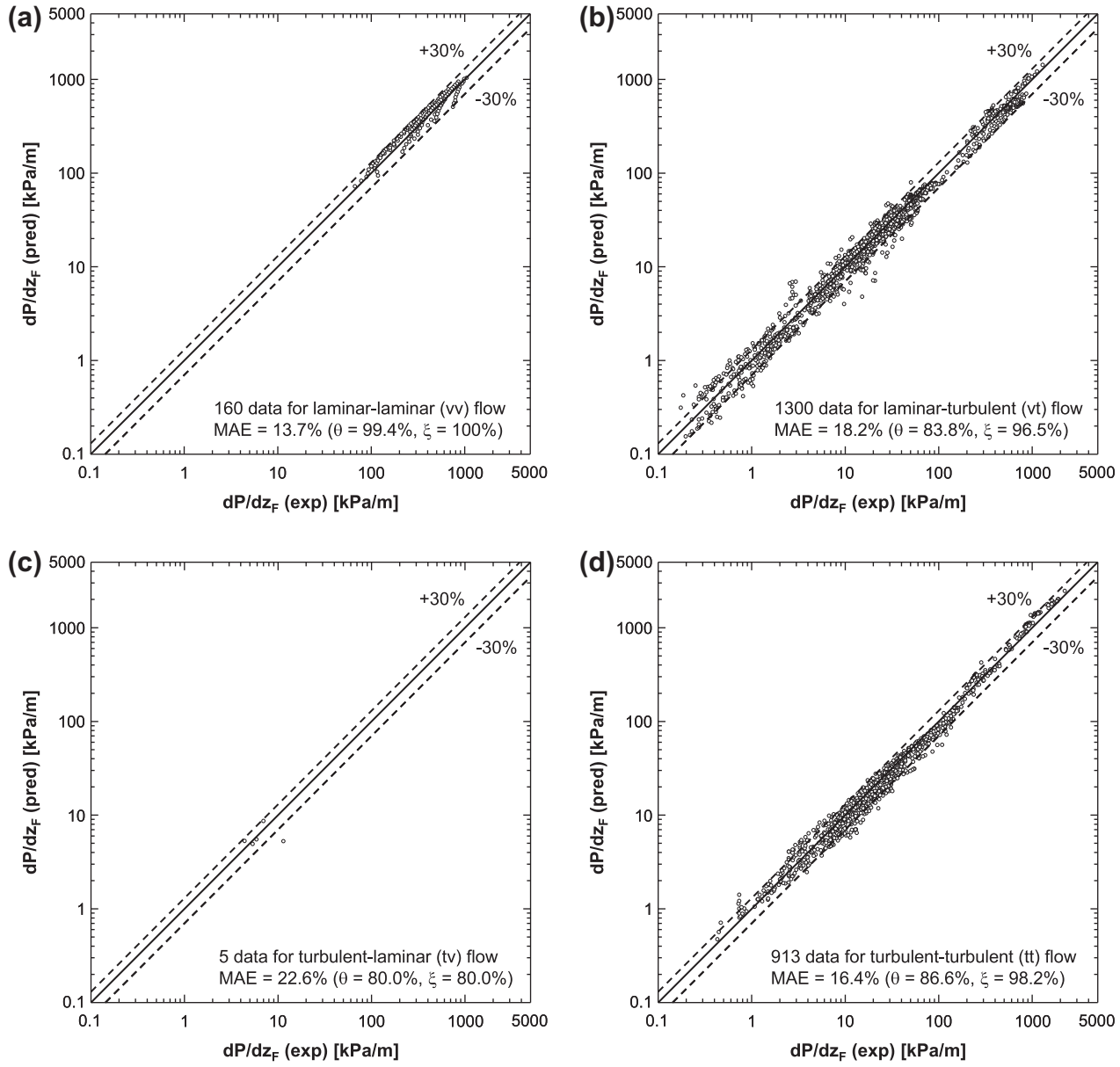

Fig. 6. Comparison of predictions of new frictional pressure drop correlation with 2378 mini/micro-channel flow boiling data points for: (a) laminar-laminar (*vv*), (b) laminar-turbulent (*vt*), (c) turbulent-laminar (*tv*), and (d) turbulent-turbulent (*tt*) flow regimes.

saturated flow boiling in mini/micro-channels based on a new consolidated database consisting of 2378 data points from 16 sources. Key findings from the study are as follows:

(1) Poor predictions of the consolidated database are achieved with all viscosity models used in conjunction with the homogeneous equilibrium model. Among all the previous predictive tools, only the Mishima and Hibiki correlation [46] shows fair predictions (MAE = 27.6%).
(2) Previous models and correlations for the frictional pressure gradient show different trends for non-boiling versus boiling mini/micro-channel flows because of fundamental differences in flow structure, especially in regards to droplet entrainment. Therefore, different predictive tools must be developed for boiling flows compared to those for non-boiling flows.
(3) A new universal correlation for frictional pressure gradient for flow boiling in mini/micro-channels is constructed by modifying the authors' previous correlation [71] for non-boiling mini/micro-channel flows with dimensionless multipliers that account for the differences in flow structure between the two flow types. The new correlation shows excellent predictive capability, with an overall MAE of 17.2% for the entire database, and 85.9% and 97.4% of the data falling within ±30% and ±50% error bands, respectively. The predictive accuracy of this correlation is also fairly even for different working fluids, and over broad ranges of hydraulic diameter, mass velocity, quality and pressure, and for both single and multiple mini/micro-channels.
(4) The new predictive correlation technique can be used with thermophysical properties based on the average saturation temperature between the channel's inlet and outlet, or on saturation temperature that varies along the channel. The two property calculation methods yield very close predictions, therefore calculations can be performed using the simpler average temperature method without compromising predictive accuracy.

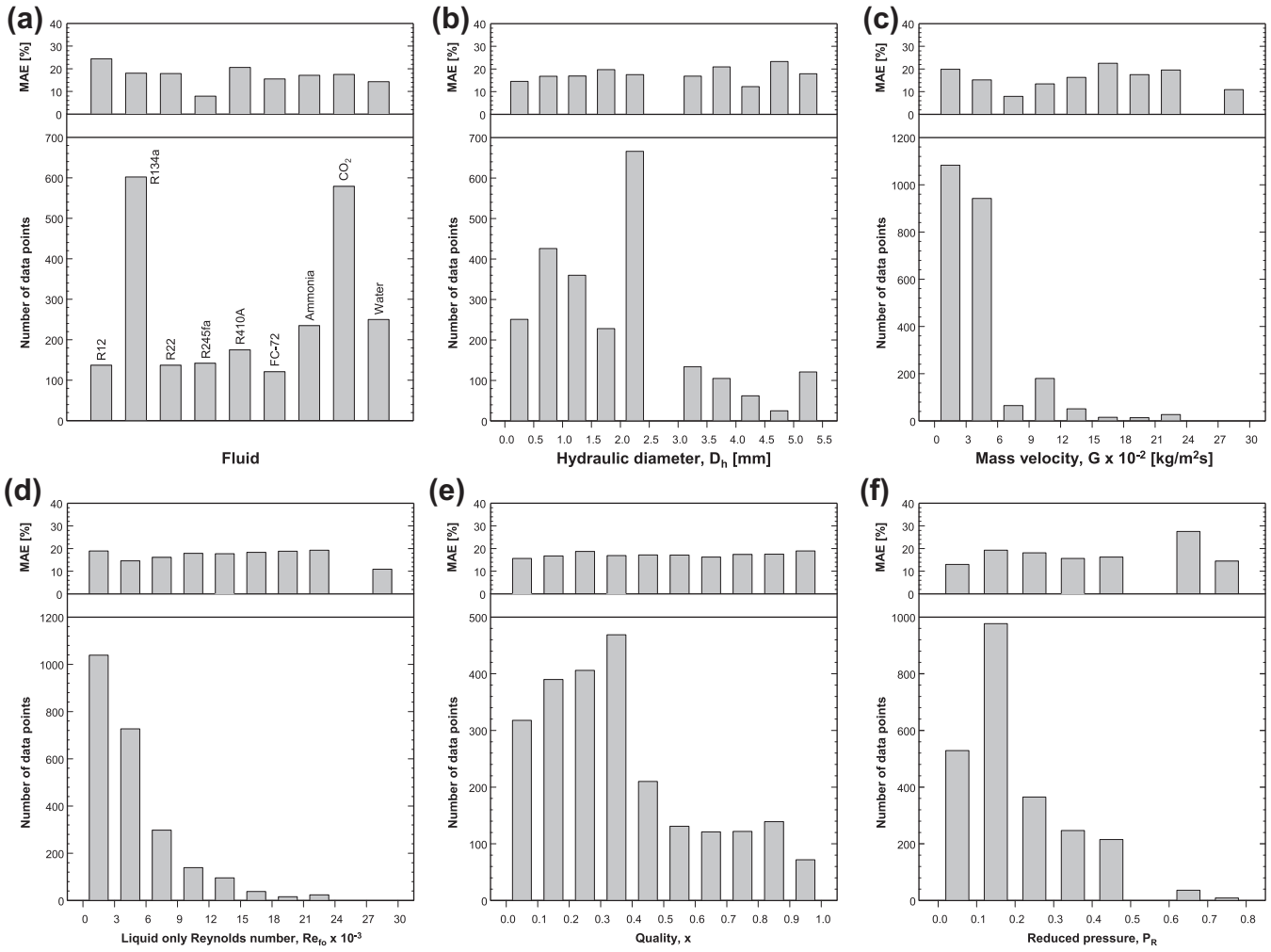

Fig. 7. Distributions of number of data points and MAE in predictions of new correlation method for entire 2378 point database relative to: (a) working fluid, (b) hydraulic diameter, (c) mass velocity, (d) liquid-only Reynolds number, (e) quality, and (f) reduced pressure.

Table 6
Comparison of individual mini/micro-channel frictional pressure drop databases with predictions of present correlation and select previous correlations.

Author(s)	Fluid(s)	D_h (mm)	Mean absolute error (%)					
			Friedel [42]	Müller-Steinhagen and Heck [43]	Wang et al. [45]	Mishima and Hibiki [46]	Li and Wu [57]	New correlation
Lezzi et al. [18]	Water	1.00	12.0	13.3	40.3	18.8	14.2	15.6
Tran [19]	R12, R134a	2.46	33.2	32.6	39.1	32.0	44.6	20.0
Pettersen [20]	CO_2	0.81	28.0	37.7	55.7	29.4	29.8	29.7
Monroe et al. [21]	R134a	1.66	20.3	19.4	33.2	24.3	33.5	24.2
Qu and Mudawar [22]	Water	0.349	360.0	88.1	68.9	18.4	21.6	13.6
Huo [23]	R134a	2.01, 4.26	51.4	61.0	42.6	31.0	67.9	20.2
Lee and Mudawar [24]	R134a	0.349	31.1	26.8	19.2	42.9	37.8	16.2
Owhaib et al. [25]	R134a	0.826, 1.224, 1.70	32.3	26.6	39.5	19.0	43.8	18.1
Hu et al. [26]	R410A	2.00, 4.18	16.0	18.8	30.3	16.5	46.3	15.2
Quibén et al. [27]	R22, R410A	3.5, 3.71, 4.88, 5.35	18.5	21.8	18.8	25.8	43.4	20.2
Ducoulombier [28]	CO_2	0.529	14.1	13.3	72.6	27.7	24.4	13.4
Tibiriçá and Ribatski [29]	R245fa	2.32	16.6	13.6	11.9	20.3	30.0	7.9
Tibiriçá et al. [30]	R134a	2.32	24.7	34.9	13.9	19.8	48.3	12.3
Wu et al. [31]	CO_2	1.42	20.2	30.6	17.2	29.5	18.9	19.0
Kharangate et al. [32]	FC72	3.33	36.7	42.5	43.0	30.5	47.2	15.5
Maqbool et al. [33]	Ammonia	1.224, 1.700	23.0	27.3	16.6	30.9	24.6	17.1
Total			47.6	31.2	35.7	27.6	34.1	17.2

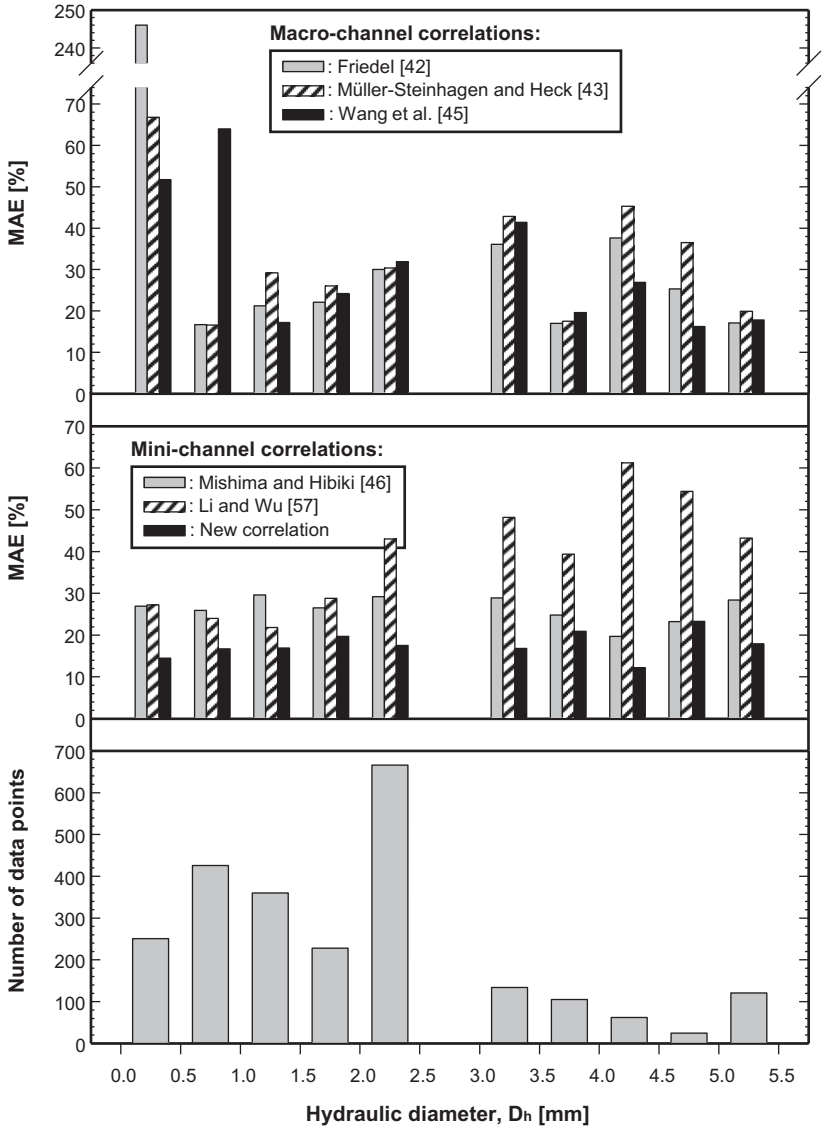

Fig. 8. Distribution of MAE in predictions of new correlation and select previous correlations for entire 2378 point database relative to hydraulic diameter.

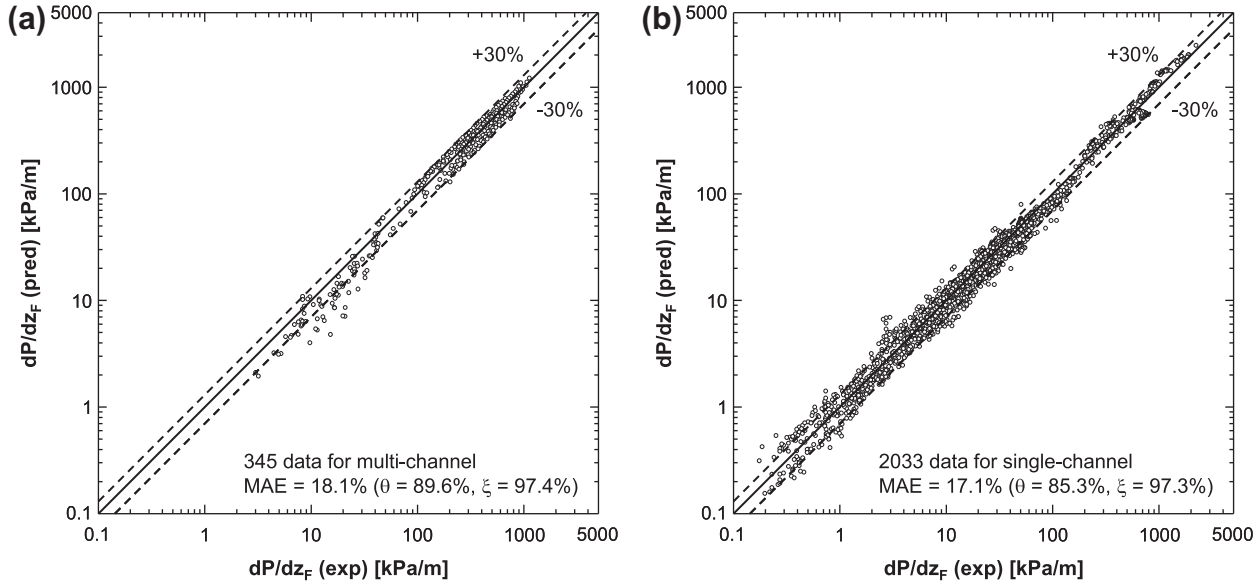

Fig. 9. Comparison of predictions of new correlation with two subsets of the new consolidated database corresponding to: (a) multi-channels and (b) single-channels.

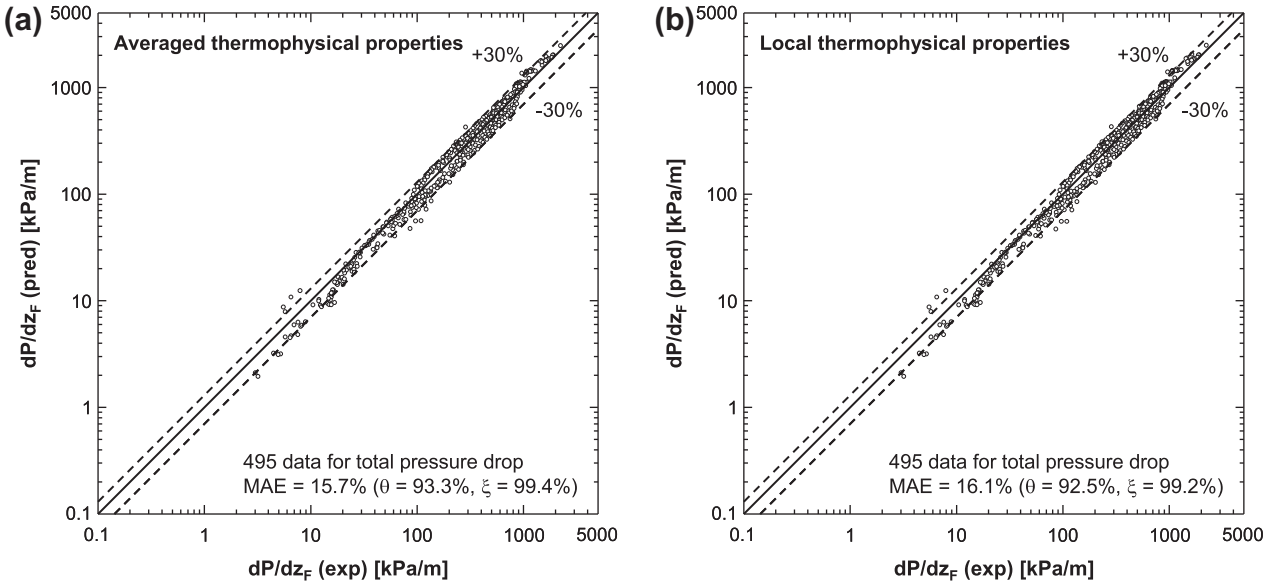

Fig. 10. Comparison of 495 total pressure drop data points with predictions of the new correlation, with the thermophysical properties based on (a) average saturation temperature between the channel's inlet and outlet, and (b) local saturation temperature.

Table 7
Influence of void fraction relation used to determine the accelerational pressure gradient on the predictions of the new frictional pressure drop correlation.

Author(s)	Fluid(s)	D_h (mm)	Mean absolute error (%)					
			Homogeneous	Lockhart and Martinelli [41]	Zivi [71]	Baroczy [78]	Rouhani and Axelsson [74]	Woldesemayat and Ghajar [75]
Lezzi et al. [18]	Water	1.00	17.6	15.3	15.6	15.4	15.5	13.8
Monroe et al. [21]	R134a	1.66	22.8	24.4	24.2	24.4	24.4	24.7
Qu and Mudawar [22]	Water	0.349	116.8	12.1	13.6	13.2	11.7	11.6
Lee and Mudawar [24]	R134a	0.349	11.3	17.2	16.2	16.9	17.0	19.4
Kharangate et al. [32]	FC72	3.33	17.0	16.5	15.5	16.2	15.2	19.5
Total			49.6	15.5	15.7	15.8	15.1	16.3

Acknowledgements

The authors are grateful for the partial support for this project from the National Aeronautics and Space Administration (NASA) under Grant No. NNX13AB01G.

References

[1] I. Mudawar, Two-phase micro-channel heat sinks: theory, applications and limitations, J. Electron. Packag. Trans. ASME 133 (2011). 041002-2.
[2] T.M. Anderson, I. Mudawar, Microelectronic cooling by enhanced pool boiling of a dielectric fluorocarbon liquid, J. Heat Transfer Trans. ASME 111 (1989) 752–759.
[3] I. Mudawar, K.A. Estes, Optimizing and predicting CHF in spray cooling of a square surface, J. Heat Transfer Trans. ASME 118 (1996) 672–680.
[4] L. Lin, R. Ponnappan, Heat transfer characteristics of spray cooling in a closed loop, Int. J. Heat Mass Transfer 46 (2003) 3737–3746.
[5] J.R. Rybicki, I. Mudawar, Single-phase and two-phase cooling characteristics of upward-facing and downward-facing sprays, Int. J. Heat Mass Transfer 49 (2006) 5–16.
[6] Y. Katto, M. Kunihiro, Study of the mechanism of burn-out in boiling system of high burn-out heat flux, Bull. JSME 16 (1973) 1357–1366.
[7] I. Mudawar, D.C. Wadsworth, Critical heat flux from a simulated electronic chip to a confined rectangular impinging jet of dielectric liquid, Int. J. Heat Mass Transfer 34 (1991) 1465–1480.
[8] D.C. Wadsworth, I. Mudawar, Enhancement of single-phase heat transfer and critical heat flux from an ultra-high-flux simulated microelectronic heat source to a rectangular impinging jet of dielectric liquid, J. Heat Transfer Trans. ASME 114 (1992) 764–768.
[9] M.E. Johns, I. Mudawar, An ultra-high power two-phase jet-impingement avionic clamshell module, J. Electron. Packag. Trans. ASME 118 (1996) 264–270.
[10] T.C. Willingham, I. Mudawar, Forced-convection boiling and critical heat flux from a linear array of discrete heat sources, Int. J. Heat Mass Transfer 35 (1992) 2879–2890.
[11] M.B. Bowers, I. Mudawar, High flux boiling in low flow rate, low pressure drop mini-channel and micro-channel heat sinks, Int. J. Heat Mass Transfer 37 (1994) 321–332.
[12] T.N. Tran, M.W. Wambsganss, D.M. France, Small circular- and rectangular-channel boiling with two refrigerants, Int. J. Multiphase Flow 22 (1996) 485–498.
[13] H.J. Lee, S.Y. Lee, Heat transfer correlation for boiling flows in small rectangular horizontal channels with low aspect ratios, Int. J. Multiphase Flow 27 (2001) 2043–2062.
[14] V. Khanikar, I. Mudawar, T. Fisher, Effects of carbon nanotube coating on flow boiling in a micro-channel, Int. J. Heat Mass Transfer 52 (2009) 3805–3817.
[15] S.M. Kim, J. Kim, I. Mudawar, Flow condensation in parallel micro-channels – Part 1: Experimental results and assessment of pressure drop correlations, Int. J. Heat Mass Transfer 55 (2012) 971–983.
[16] W. Qu, I. Mudawar, Transport phenomena in two-phase micro-channel heat sinks, J. Electron. Packag. Trans. ASME 126 (2004) 213–224.
[17] J. Lee, I. Mudawar, Two-phase flow in high-heat-flux micro-channel heat sink for refrigeration cooling applications: Part II – heat transfer characteristics, Int. J. Heat Mass Transfer 48 (2005) 941–955.
[18] A.M. Lezzi, A. Niro, G.P. Beretta, Experimental data on CHF for forced convection water boiling in long horizontal capillary tubes, in: Proceedings of the Tenth International Heat Transfer Conference, UK, 7, 1994, pp. 491–496.
[19] T.N. Tran, Pressure drop and heat transfer study of two-phase flow in small channels, Ph.D thesis, Texas Tech University, TX, 1998.
[20] J. Pettersen, Flow vaporization of CO_2 in microchannel tubes, Ph.D Thesis, Norwegian University of Science and Technology, Norway, 2002.
[21] C.A. Monroe, T.A. Newell, J.C. Chato, An experimental investigation of pressure drop and heat transfer in internally enhanced aluminum microchannels, Report No. ACRC TR-213, Air Conditioning and Refrigeration Center, University of Illinois at Urbana-Champaign, 2003.
[22] W. Qu, I. Mudawar, Measurement and prediction of pressure drop in two-phase micro-channel heat sinks, Int. J. Heat Mass Transfer 46 (2003) 2737–2753.

[23] X. Huo, Experimental study of flow boiling heat transfer in small diameter tubes, Ph.D thesis, London South Bank University, UK, 2005.
[24] J. Lee, I. Mudawar, Two-phase flow in high-heat-flux micro-channel heat sink for refrigeration cooling applications: Part I – pressure drop characteristics, Int. J. Heat Mass Transfer 48 (2005) 928–940.
[25] W. Owhaib, C. Martín-Callizo, B. Palm, Two-phase flow pressure drop of R-134A in a vertical circular mini/micro channel, in: ASME Sixth International Conference on Nanochannels, Microchannels, and Minichannels, Germany, ICNMM2008-62243, 2008, pp. 343–353.
[26] H.T. Hu, G.L. Ding, X.C. Huang, B. Deng, Y.F. Gao, Pressure drop during horizontal flow boiling of R410A/oil mixture in 5 mm and 3 mm smooth tubes, Appl. Therm. Eng. 29 (2009) 3353–3365.
[27] J.M. Quibén, L. Cheng, R. Lima, J.R. Thome, Flow boiling in horizontal flattened tubes: Part I – two-phase frictional pressure drop results and model, Int. J. Heat Mass Transfer 52 (2009) 3634–3644.
[28] M. Ducoulombier, Ebullition convective du dioxyde de carbone - étude expérimentale en micro-canal, Ph.D thesis, Institut National des Sciences Appliquées (INSA) de Lyon, France, 2010.
[29] C.B. Tibiriçá, G. Ribatski, Two-phase frictional pressure drop and flow boiling heat transfer for R245fa in a 2.32-mm tube, Heat Transfer Eng. 32 (2011) 1139–1149.
[30] C.B. Tibiriçá, J.D. Silva, G. Ribatski, Experimental investigation of flow boiling pressure drop of R134A in a microscale horizontal smooth tube, J. Therm. Sci. Eng. Appl. Trans. ASME 3 (2011) 011006.
[31] J. Wu, T. Koettig, Ch. Franke, D. Helmer, T. Eisel, F. Haug, J. Bremer, Investigation of heat transfer and pressure drop of CO_2 two-phase flow in a horizontal minichannel, Int. J. Heat Mass Transfer 54 (2011) 2154–2162.
[32] C.R. Kharangate, I. Mudawar, M.M. Hasan, Experimental and theoretical study of critical heat flux in vertical upflow with inlet vapor void, Int. J. Heat Mass Transfer 55 (2012) 360–374.
[33] M.H. Maqbool, B. Palm, R. Khodabandeh, Flow boiling of ammonia in vertical small diameter tubes: two phase frictional pressure drop results and assessment of prediction methods, Int. J. Therm. Sci. 54 (2012) 1–12.
[34] W.H. McAdams, W.K. Woods, L.C. Heroman, Vaporization inside horizontal tubes, II. Benzene–oil mixture, Trans. ASME 64 (1942) 193–200.
[35] W.W. Akers, H.A. Deans, O.K. Crosser, Condensing heat transfer within horizontal tubes, Chem. Eng. Prog. 54 (1958) 89–90.
[36] A. Cicchitti, C. Lombardi, M. Silvestri, G. Soldaini, R. Zavalluilli, Two-phase cooling experiments-pressure drop, heat transfer and burnout measurements, Energia nucleare 7 (1960) 407–425.
[37] W.L. Owens, Two-phase pressure gradient. in: Int. Dev. Heat Transfer, Pt. II., ASME, New York, 1961.
[38] A.E. Dukler, M. Wicks, R.G. Cleaveland, Pressure drop and hold up in two-phase flow, AIChE J. 10 (1964) 38–51.
[39] D.R.H. Beattie, P.B. Whalley, A simple two-phase frictional pressure drop calculation method, Int. J. Multiphase Flow 8 (1982) 83–87.
[40] S. Lin, C.C.K. Kwok, R.Y. Li, Z.H. Chen, Z.Y. Chen, Local frictional pressure drop during vaporization of R-12 through capillary tubes, Int. J. Multiphase Flow 17 (1991) 95–102.
[41] R.W. Lockhart, R.C. Martinelli, Proposed correlation of data for isothermal two-phase, two-component flow in pipes, Chem. Eng. Prog. 45 (1949) 39–48.
[42] L. Friedel, Improved friction pressure drop correlations for horizontal and vertical two-phase pipe flow, in: European Two-phase Group Meeting, Ispra, Italy, 1979, Paper E2.
[43] H. Müller-Steinhagen, K. Heck, A simple friction pressure drop correlation for two-phase flow in pipes, Chem. Eng. Process. 20 (1986) 297–308.
[44] D.S. Jung, R. Radermacher, Prediction of pressure drop during horizontal annular flow boiling of pure and mixed refrigerants, Int. J. Heat Mass Transfer 32 (1989) 2435–2446.
[45] C.C. Wang, C.S. Chiang, D.C. Lu, Visual observation of two-phase flow pattern of R-22, R-134a, and R-407C in a 6.5-mm smooth tube, Exp. Therm. Fluid Sci. 15 (1997) 395–405.
[46] K. Mishima, T. Hibiki, Some characteristics of air–water two-phase flow in small diameter vertical tubes, Int. J. Multiphase Flow 22 (1996) 703–712.
[47] C.Y. Yang, R.L. Webb, Friction pressure drop of R-12 in small hydraulic diameter extruded aluminum tubes with and without micro-fins, Int. J. Heat Mass Transfer 39 (1996) 801–809.
[48] Y.Y. Yan, T.F. Lin, Evaporation heat transfer and pressure drop of refrigerant R-134a in a small pipe, Int. J. Heat Mass Transfer 41 (1998) 4183–4194.
[49] T.N. Tran, M.C. Chyu, M.W. Wambsganss, D.M. France, Two-phase pressure drop of refrigerants during flow boiling in small channels: an experimental investigation and correlation development, Int. J. Multiphase Flow 26 (2000) 1739–1754.
[50] I.Y. Chen, K.S. Yang, Y.J. Chang, C.C. Wang, Two-phase pressure drop of air–water and R-410A in small horizontal tubes, Int. J. Multiphase Flow 27 (2001) 1293–1299.
[51] H.J. Lee, S.Y. Lee, Pressure drop correlations for two-phase flow within horizontal rectangular channels with small heights, Int. J. Multiphase Flow 27 (2001) 783–796.
[52] W. Yu, D.M. France, M.W. Wambsganss, J.R. Hull, Two-phase pressure drop, boiling heat transfer, and critical heat flux to water in a small-diameter horizontal tube, Int. J. Multiphase Flow 28 (2002) 927–941.
[53] Y.W. Hwang, M.S. Kim, The pressure drop in microtubes and the correlation development, Int. J. Heat Mass Transfer 49 (2006) 1804–1812.
[54] L. Sun, K. Mishima, Evaluation analysis of prediction methods for two-phase flow pressure drop in mini-channels, Int. J. Multiphase Flow 35 (2009) 47–54.
[55] W. Li, Z. Wu, A general correlation for adiabatic two-phase pressure drop in micro/mini-channels, Int. J. Heat Mass Transfer 53 (2010) 2732–2739.
[56] W. Zhang, T. Hibiki, K. Mishima, Correlations of two-phase frictional pressure drop and void fraction in mini-channel, Int. J. Heat Mass Transfer 53 (2010) 453–465.
[57] W. Li, Z. Wu, Generalized adiabatic pressure drop correlations in evaporative micro/mini-channels, Exp. Therm. Fluid Sci. 35 (2011) 866–872.
[58] I. Mudawar, A.H. Howard, C.O. Gersey, An analytical model for near-saturated pool boiling CHF on vertical surfaces, Int. J. Heat Mass Transfer 40 (1997) 2327–2339.
[59] A.H. Howard, I. Mudawar, Orientation effects on pool boiling CHF and modeling of CHF for near-vertical surfaces, Int. J. Heat Mass Transfer 42 (1999) 1665–1688.
[60] J.E. Galloway, I. Mudawar, CHF mechanism in flow boiling from a short heated wall – Part 1. Examination of near-wall conditions with the aid of photomicrography and high-speed video imaging, Int. J. Heat Mass Transfer 36 (1993) 2511–2526.
[61] J.E. Galloway, I. Mudawar, CHF mechanism in flow boiling from a short heated wall – Part 2. Theoretical CHF model, Int. J. Heat Mass Transfer 36 (1993) 2527–2540.
[62] C.O. Gersey, I. Mudawar, Effects of heater length and orientation on the trigger mechanism for near-saturated flow boiling critical heat flux – I. Photographic study and statistical characterization of the near-wall interfacial features, Int. J. Heat Mass Transfer 38 (1995) 629–641.
[63] C.O. Gersey, I. Mudawar, Effects of heater length and orientation on the trigger mechanism for near-saturated flow boiling critical heat flux – II. Critical heat flux model, Int. J. Heat Mass Transfer 38 (1995) 643–654.
[64] J.C. Sturgis, I. Mudawar, Critical heat flux in a long, rectangular channel subjected to onesided heating – I. Flow visualization, Int. J. Heat Mass Transfer 42 (1999) 1835–1847.
[65] J.C. Sturgis, I. Mudawar, Critical heat flux in a long, rectangular channel subjected to onesided heating – II. Analysis of critical heat flux data, Int. J. Heat Mass Transfer 42 (1999) 1849–1862.
[66] S.M. Kim, I. Mudawar, Theoretical model for annular flow condensation in rectangular micro-channels, Int. J. Heat Mass Transfer 55 (2012) 958–970.
[67] I. Mudawar, M.B. Bowers, Ultra-high critical heat flux (CHF) for subcooled water flow boiling – I. CHF data and parametric effects for small diameter tubes, Int. J. Heat Mass Transfer 42 (1999) 1405–1428.
[68] D.D. Hall, I. Mudawar, Ultra-high critical heat flux (CHF) for subcooled water flow boiling – II. High-CHF database and design parameters, Int. J. Heat Mass Transfer 42 (1999) 1429–1456.
[69] D.D. Hall, I. Mudawar, Critical heat flux (CHF) for water flow in tubes – I. Compilation and assessment of world CHF data, Int. J. Heat Mass Transfer 43 (2000) 2573–2604.
[70] D.D. Hall, I. Mudawar, Critical heat flux (CHF) for water flow in tubes – II. Subcooled CHF correlations, Int. J. Heat Mass Transfer 43 (2000) 2605–2640.
[71] S.M. Kim, I. Mudawar, Universal approach to predicting two-phase frictional pressure drop for adiabatic and condensing mini/micro-channel flows, Int. J. Heat Mass Transfer 55 (2012) 3246–3261.
[72] S.M. Zivi, Estimation of steady-state steam void-fraction by means of the principle of minimum entropy production, J. Heat Transfer Trans. ASME 86 (1964) 247–252.
[73] F.P. Incropera, D.P. Dewitt, Fundamentals of Heat and Mass Transfer, fifth ed., Wiley, New York, 2002.
[74] R.K. Shah, A.L. London, Laminar Flow Forced Convection in Ducts: A Source Book for Compact Heat Exchanger Analytical Data, Academic press, New York, 1978. Supl. 1.
[75] S.Z. Rouhani, E. Axelsson, Calculation of void volume fraction in the subcooled and quality boiling region, Int. J. Heat Mass Transfer 13 (1970) 393.
[76] M.A. Woldesemayat, A.J. Ghajar, Comparison of void fraction correlations for different flow patterns in horizontal and upward inclined pipes, Int. J. Multiphase Flow 33 (2007) 347–370.
[77] E.W. Lemmon, M.L. Huber, M.O. McLinden, Reference fluid thermodynamic and transport properties – REFPROP Version 8.0, NIST, MD, 2007.
[78] C.J. Baroczy, Correlation of liquid fraction in two-phase flow with applications to liquid metals, Chem. Eng. Prog. 61 (1965) 179–191.
[79] S.M. Kim, I. Mudawar, Flow condensation in parallel micro-channels – Part 2: Heat transfer results and correlation technique, Int. J. Heat Mass Transfer 55 (2012) 984–994.
[80] J.A. Shmerler, I. Mudawar, Local heat transfer coefficient in wavy free-falling turbulent liquid films undergoing uniform sensible heating, Int. J. Heat Mass Transfer 31 (1988) 67–77.
[81] J.A. Shmerler, I. Mudawar, Local evaporative heat transfer coefficient in turbulent free-falling liquid films, Int. J. Heat Mass Transfer 31 (1988) 731–742.
[82] T.H. Lyu, I. Mudawar, Statistical investigation of the relationship between interfacial waviness and sensible heat transfer to a falling liquid film, Int. J. Heat Mass Transfer 34 (1991) 1451–1464.
[83] T.H. Lyu, I. Mudawar, Determination of wave-induced fluctuations of wall temperature and convective heat transfer coefficient in the heating of a turbulent falling liquid film, Int. J. Heat Mass Transfer 34 (1991) 2521–2534.

[84] I. Mudawar, R.A. Houpt, Mass and momentum transport in falling liquid films laminarized at relatively high Reynolds numbers, Int. J. Heat Mass Transfer 36 (1993) 3437–3448.
[85] I. Mudawar, R.A. Houpt, Measurement of mass and momentum transport in wavy-laminar falling liquid films, Int. J. Heat Mass Transfer 36 (1993) 4151–4162.
[86] I. Mudawar, M.A. El-Masri, Momentum and heat transfer across freely-falling turbulent liquid films, Int. J. Multiphase Flow 12 (1986) 771–790.
[87] J.E. Koskie, I. Mudawar, W.G. Tiederman, Parallel-wire probes for measurement of thick liquid films, Int. J. Multiphase Flow 15 (1989) 521–530.